体制御因子を欠損するPNH赤血球が，補体の活性化に伴い血管内溶血を起こす。最近，GPI-AP合成に関わる他の遺伝子*PIGT*の変異によっても，PNHを発症することが報告された[12]。症例は典型的なPNH症状を呈していたが，*PIGA*に変異がみつからず，GPI-AP合成に関わる遺伝子群の全エクソンシークエンスを行ったところ，GPIトランスアミダーゼの構成成分である*PIGT*遺伝子において，ヘテロの先天性変異にPNHタイプ血球特異的な体細胞突然変異が付加されていることが証明された。

PNHクローンの拡大には，動物実験の成績から*PIGA*遺伝子変異だけでは不十分であることが判明している[13~17]。再生不良性貧血（aplastic anemia, AA）を代表とする造血不全疾患としばしば合併・相互移行すること，AA患者の約50％に微少なPNH血球（＞0.003％）が検出されることなど[18]，AAとの深い関連性から，AAにみられるような免疫学的機構がPNHクローンの相対的増加（選択機序）に関与しているとされる。すなわち，造血障害を引き起こす免疫学的傷害のターゲットとしてGPI-APを介していれば，これを発現する正常幹細胞は傷害されるのに対し，PNH幹細胞はこの傷害を免れることになり，PNHクローンの拡大機序を説明する上で大変魅力的な説である。以前からLuzzattoらは，この説を説明する一つの機序として，PNH患者において類似のTCRVβを発現するNKT細胞（CD8＋，CD57＋）集団の存在を報告していた[19]。彼らは，化学合成した血流型トリパノソーマ由来GPIとヒトGPIを用いた実験から，GPIがCD1dによってPNH患者のNKT細胞に提示され活性化することを示した[20]。GPIアンカー欠損細胞は，一部の健常者において微量ではあるが存在することや[21]，PNH患者では，複数のGPIアンカー欠損クローンが存在することが知られており[22]，1つのクローンが拡大していても，他のクローンは，必ずしも拡大しているとは限らないことから，*PIGA*の変異，免疫学的選択に加え，さらに何らかの付加的異常の関与が疑われていた。

井上らは，脂肪種や子宮筋腫等の良性腫瘍の原因遺伝子である*High-mobility group AT-hook 2*（*HMGA2*）が，2例でPNHクローンに異所性に発現し，腫瘍性性格を与えている事を報告していた[23]。その後，βサラセミア患者の骨髄細胞に正常なβグロビン遺伝子をレンチウイルスベクターを用いて遺伝子治療を行ったところ，βグロビン遺伝子を含むベクターは*HMGA2*遺伝子のイントロン3に挿入され，*HMGA2*遺伝子が異所性に発現した結果，クローン性の造血が回復し，輸血も不要となった[24]。さらに，*HMGA2*遺伝子を過剰発現したマウスを作成すると，造血幹細胞/前駆細胞の段階でクローン性の拡大を伴う造血能を獲得していることが示された[25]。これらのことは，*HMGA2*遺伝子の高発現がクローン性増殖をもたらすことを直接証明するもので，今後のさらなる解析が注目される。

PNHの治療

PNHは補体介在性の血管内溶血，骨髄不全および血栓症を3大症状とするが，それぞれの症状の程度とその全体のバランスは症例ごとに様々である。PNHの根治療法は造血幹細胞移植であるが，疾患の希少性もあり明確な基準はない（致命的な血栓症や重度の造血不全が主な適応と考えられる）。前述の如く，PNH患者は，3大症状のみならず，腹痛，嚥下障害，男性機能不全など多彩な症状を呈するが，これらの症状が溶血に起因していることが近年明らかになり，溶血を抑制することがPNH患者の多くの症状やQoLを著しく改善すると期待されるようになった[10]。このような潮流の中で，PNH溶血に対する治療薬として，新規補体阻害剤（eculizumab）が開発された。

1. 新規補体阻害剤eculizumab（Soliris®，アレクシオンファーマ）の開発

Eculizumabは，ヒトC5上のエピトープと結合し，C5転換酵素の作用を阻害する（Fig. 1）[26]。C5と特異的に結合することにより，炎症性メディエータであるC5a（アナフィラトキシン）の放出を阻害するとともに，C5b（膜侵襲蛋白）に引き続く膜破壊性のC5b-9複合体の生成を阻害するが，病原体のオプソニン化や免疫複合体の除去等には影響を与えない。結合部位である相補性決定領域（complementarity determining region, CDR）はマウスとヒトのキメラになっている。一方，重鎖定常領域（heavy-chain constant region, CH）1にヒトIgG2を，CH2と3にヒトIgG4を用いることにより，Fcレセプターに結合したり補体を活性化したりしないように工夫されているのが特徴である。

本邦での第2相試験AEGISに先立ち3つの臨床試験が海外で先行して行われた。英国で行われた第2相オープンラベルパイロット試験で，溶血に対する劇的な効果が示された[27,28]。引き続き欧米で行われた，有効性を判定するプラセボ対照二重盲検第3相試験TRIUMPH[29]と安全性を判定する非盲検第3相試験SHEPHERD（97例）[30]があり，いずれも共通の継続試験に入り（TRIUMPHのプラセボ群も含む），多くの欧米諸国で承認に至っている。本邦でもAEGIS試験（29例）が2008年に開始され，これまでの成績と同等の有効性と安全性が示され，2010年4月に承認に至った[2,31]。投与方法は25～45分点滴静注で，600 mgを週1回4週続けて投与し，5週目に900 mgを投与，その後2週毎に900 mg

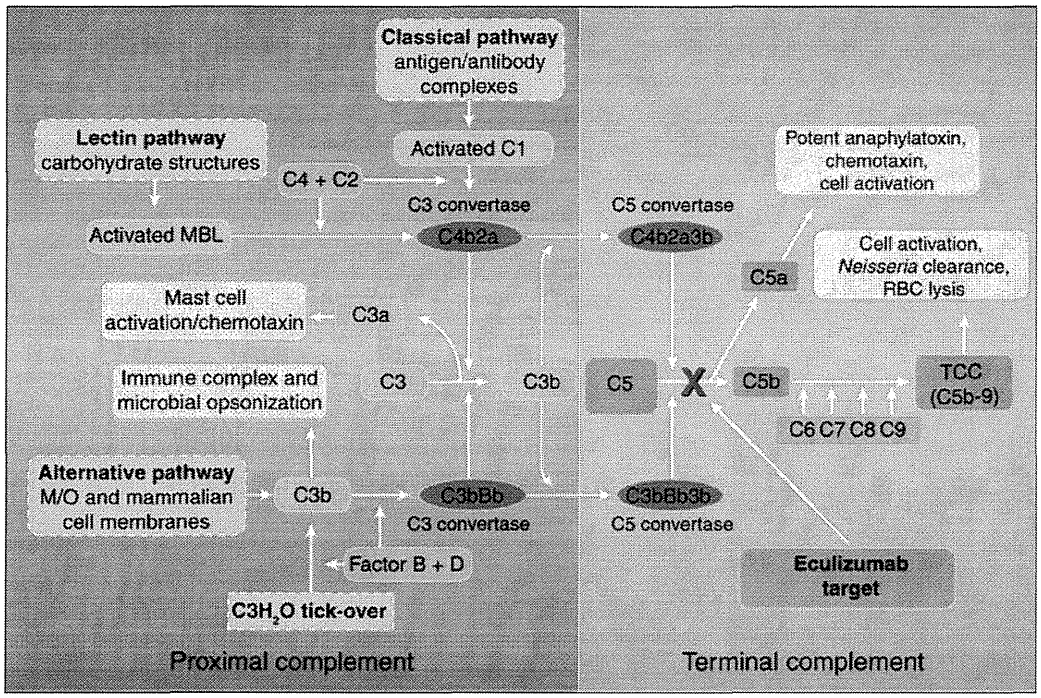

Fig. 1 The complement pathway and these regulatory factors. Eculizumab targets blockade of complement protein C5[26].

を継続投与する。投与に先立ち髄膜炎菌に対するワクチン接種が推奨される。

2. 本邦 AEGIS 試験における臨床成績

本邦では 12 週間の AEGIS 試験と[31]，引き続き 2 年間の継続試験が行われた[2]。AEGIS 試験には 29 人が参加し，溶血の指標である LDH の平均値は，投与前値の 1,845 U/*l* から投与 12 週後には 399 U/*l* まで低下した（P<0.001）（Fig. 2A）。LDH の低下は eculizumab 投与後 1 週目から見られ，投与期間中その効果は持続した。ヘモグロビン値も投与前中央値 7.6 g/d*l* に対し，投与後 9 g/d*l* と有意な改善（P<0.001）を認め，輸血量も投与前後 12 週で比較すると，5.2 U（平均）から 1.5 U（平均）へと有意に減少した（P=0.006）。投与前 12 週に輸血歴のあった 21 例のうち，14 例（66%）は投与後 12 週に輸血は不要となった（P=0.001）。このように輸血量は有意に減少するものの，輸血依存から脱却できない症例も存在することがわかった。疲労度について FACIT 疲労スコアを用いて調べると，投与後速やかに効果を認め，臨床的に有意な改善とされる 3 ポイント以上の改善を，1 週目に 38%，2 週目に 62%，12 週目に 66%の症例に認めた（Fig. 2B）。PNH 患者の慢性溶血による慢性腎臓病（CKD）は重要な予後因子であるが，CKD の病期分類を行うと，66%（19/29）の症例に CKD を認めた（Fig. 2C）。eculizumab 投与後 12 週で，19 例の CKD 合併症例のうち 12 例（63%）において病期の改善を認めた（Fig. 2D）。この改善効果は，軽度の CKD（1～2 期）においてより顕著であった。5 例において血栓・塞栓の既往を認めたが，12 週の投与期間中に血栓・塞栓を発症した症例はなかった。29 例中 11 例（38%）において，D ダイマーの投与前値が高値であったが，5 例（45%）は投与後 12 週で正常値に復した（P<0.001）。血栓症の予防効果については，欧米例でより顕著であった。欧米で行われた 3 つの臨床試験を合わせた継続試験における，治療前後の血栓症発症頻度に関する後方視的研究によって，eculizumab による血栓症予防効果を調べた[32]。継続試験の 195 例について，治療前後で血栓症発症頻度（事象/100 症例-年）を比較すると，治療前 7.4 に対し，治療後 1.1 と有意な予防効果を認めた（P<0.001）。

有害事象のほとんど（98.3%）は，軽度～中等度であった。試験期間中の死亡例，有害事象による脱落例，髄膜炎感染症，重篤な血管病変，溶血発作などの発症はなかった。重篤な有害事象としては，明らかな関連性が指摘できない発熱が 1 例報告されたのみであった。主な副作用としては，頭痛（52%），鼻咽頭炎（41%）及び悪心（21%）などで，頭痛を訴えた 15 例のうち 14 例は投与開始後 24 時間以内に発現した。すべての頭痛は軽度～中等度で，通常の頭痛薬で対処可能であった。2 年間

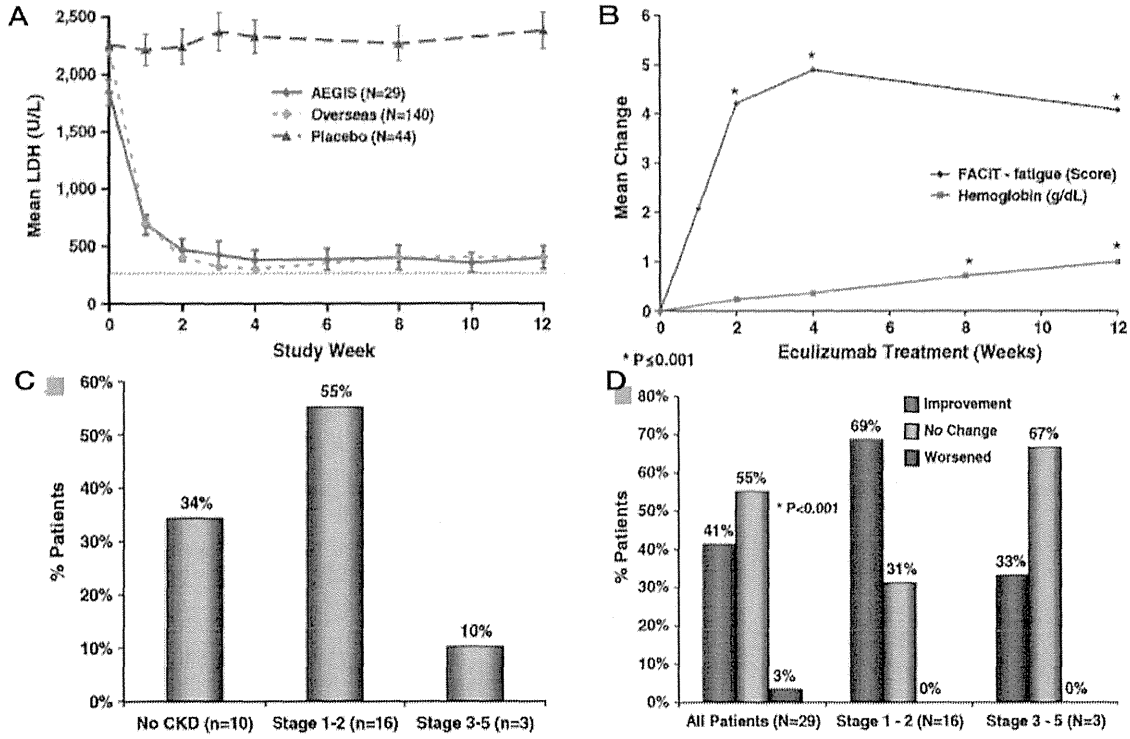

Fig. 2　Clinical improvement by Eculizumab[31]. A) Effects on hemolytic marker LDH. B) Improvement in FACIT fatigue score. C) Chronic kidney diseases (CKD) in Japanese PNH patients. D) Improvement in CKD stage.

に及ぶ継続試験の結果も合わせて本邦の結果は，これまでの欧米の結果と同等であり，本邦における eculizumab の有効性と，長期使用の安全性，忍容性が確認された。2002 年に英国でパイロット試験が開始され，既に 10 年以上経過している。英国で治療された 79 例について累積生存率を解析したところ，年齢，性別対応正常コントロール群と差がなかった。溶血・血栓症状より造血不全症状の強い本邦例においてはどうかという検証をする必要はあるが，eculizumab により PNH 患者の生活は一変したと言っても過言ではない。

Eculizumab 不応例と C5 遺伝子多型

1. 本邦第 2 相試験 AEGIS と eculizumab 不応例

本邦 AEGIS 試験においてもこれまでの成績同様，顕著な溶血抑制効果に加え，腎機能改善効果，血栓予防効果，QOL 改善効果など様々な臨床効果が確認されたが，溶血の指標である血清 LDH 値が全く低下しない不応症を 29 例中 2 例に認めた（Fig. 3A）[31]。Eculizumab の血中反応濃度である 35 μg/m*l* は，いずれの eculizumab 投与血清（ピーク/トラフ）においても維持されていた[4]。これら血清による *in vitro* 溶血試験では，反応例で投与直後より抑制されたのに対し，不応 2 例では抑制されなかった（Fig. 3B）[4]。そこで，eculizumab 投与前血清に eculizumab 添加による濃度勾配溶血試験を行ったところ，健常人と反応例は 12.5 μg/m*l* で抑制されたが，不応 2 例では 2,000 μg/m*l* の高濃度でも抑制されなかった（Fig. 3C）[4]。Eculizumab と C5 結合部位の異なる抗体 N19/8 を用いた溶血試験では，不応 2 例も健常人や反応例と同様に抑制された（Fig. 3D）[4]。そこで，C5 遺伝子の塩基配列を決定したところ，不応症のエクソン 21 にヘテロ変異 c.2654 G>A を認め，p.Arg885His 多型が予測されたが，反応 7 例には同変異を認めなかった[4]。

2. 変異 C5 蛋白の機能特性[4]

遺伝子組み換え型 C5 蛋白を作成し，蛋白機能特性を解析した。野生型 C5，変異型 C5 はいずれも *in vitro* で十分な溶血活性を示したが，eculizumab と結合し，eculizumab によって溶血が抑制されたのは野生型 C5 のみであった（Fig. 4）。N19/8 抗体に対しては野生型，変異型いずれの C5 によって構築された溶血も同様に抑制された。

3. アルゼンチン不応症例[4]

アジア系アルゼンチン原住民の eculizumab 不応症患者の紹介を受け，同様に解析を行ったところ，きわめて類似するヘテロ変異 c.2653C>T を認め，p.Arg885Cys

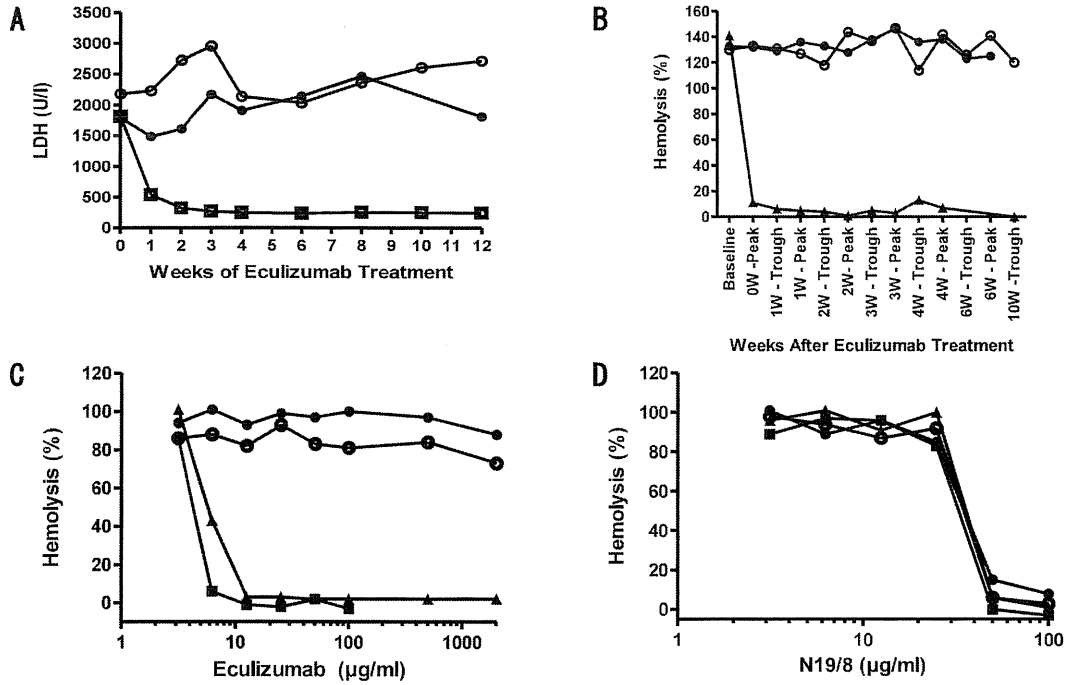

Fig. 3 Analysis of 2 poor responders in AEGES clinical study[4]. A) Effects on hemolytic marker LDH. B) *In vitro* hemolytic activity using serum on Eculizumab (peak/trough). C) *In vitro* hemolytic activity using exogenous Eculizumab. D) *In vitro* hemolytic activity using a different anti-C5 antibody (N19/8). (●)(○), poor responders; (□), responder in AEGIS; (▲), typical responder; (■), healthy individual

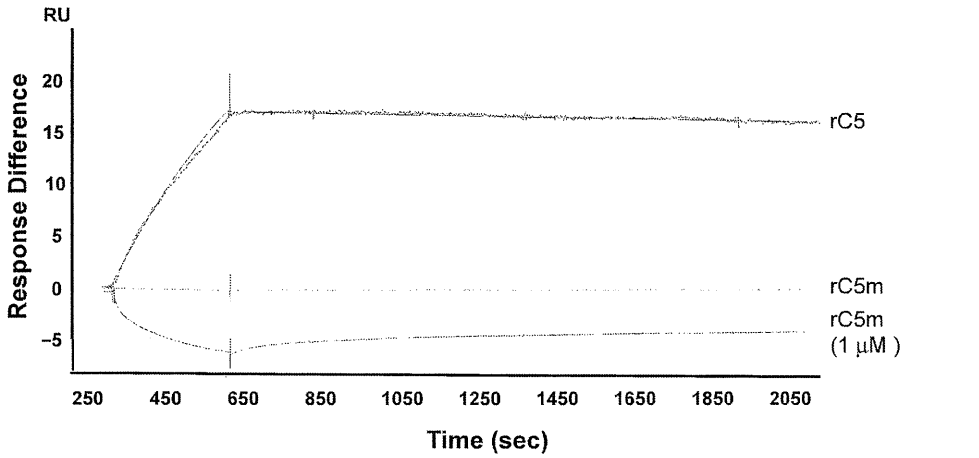

Fig. 4 Effect of Japanese C5 polymorphism on the functional properties of C5[4]. (rC5),wild type; (rC5 m),mutant

が予測された。

4. C5(Arg885)変異の人種間スクリーニング (Table 1)[4]

本邦で eculizumab 承認後，さらに 9 例の不応症が確認され，全例で c.2654 G>A ヘテロ変異を確認した。日本人の健常人 288 人（男性 200 人，女性 88 人）で c.2654 G>A 変異のスクリーニングを行ったところ，ヘテロ変異を 288 人中 10 人（3.5%）に認めた。これは本邦 PNH 患者の変異保有率（345 例中 11 例；3.2%）と同程度であった。さらに，この多型は中国漢民族集団においても確認された。一方，アルゼンチン患者に見いだされた c.2653C>T 変異は，100 例前後の解析では英国人，中国漢民族，メキシコ原住民いずれにおいても検出されず，保有率がさらに低い可能性が示唆された。

5. Eculizumab 奏効不良と新規候補薬剤の開発

Eculizumab は PNH の血管内溶血を強力に抑制するものの，貧血ならびに輸血依存に対する効果は，限定的に留まる症例が一定数存在する。この主たる原因として，PNH 患者が本来持ち合わせている造血不全と，新たに発現した血管外溶血の存在が指摘されている[33]。すなわち，eculizumab を投与したことにより，前期補体成分 C3 断片である C3b が PNH 血球へ蓄積し，オプソニン化を介して血管外溶血が顕在化したものと理解される (Fig. 1)。この血管外溶血を克服する意味合いも含め，補体レセプター 2 (CR2/CD21) と H 因子の融合蛋白である TT30[34, 35]，C3 に結合しその機能を阻害する環状ペプチドであるコンプスタチンの誘導体 Cp40[6]，遺伝性血管性浮腫 (HAE) の治療薬として承認されている C1 インヒビター (C1INH)[5] などの候補薬剤による，血管内溶血抑制に加え C3 蓄積抑制効果も報告されており，これらの薬剤は eculizumab 不応症にも有効と考えられ，今後の臨床開発への進展が期待される。

おわりに

日本人 (アジア) 固有の C5 遺伝子多型 c.2654 G>A は，C5 補体活性自体には異常をきたさないものの，eculizumab の結合に影響する重要な変異であり，その結果，薬剤不応性をきたすと考えられた。このことは，標的蛋白における遺伝子多型が，様々な疾患に対して繁用されている抗体療法の反応性を検討する上で，極めて重要な現象であることを示唆している (Fig. 5)。本邦における eculizumab の使用拡大に伴い，不応症も増加している。残念ながら，2 名の患者は，PNH 関連合併症により既に亡くなられた。また，残りの患者の多くも，

Table 1 Ethnic distribution of genetic variants in C5.

Origin	Analyzed numbers	Japanese c. 2654G>A p. Arg885His	Argentinianc. 2653C>T p. Arg885Cys
Japanese	288	10 (3.5%)	–
British from England and Scotland	100	0 (0%)	0 (0%)
Han Chinese	120	1 (0.8%)	(0%)
Native Mexican American	90	0 (0%)	0 (0%)

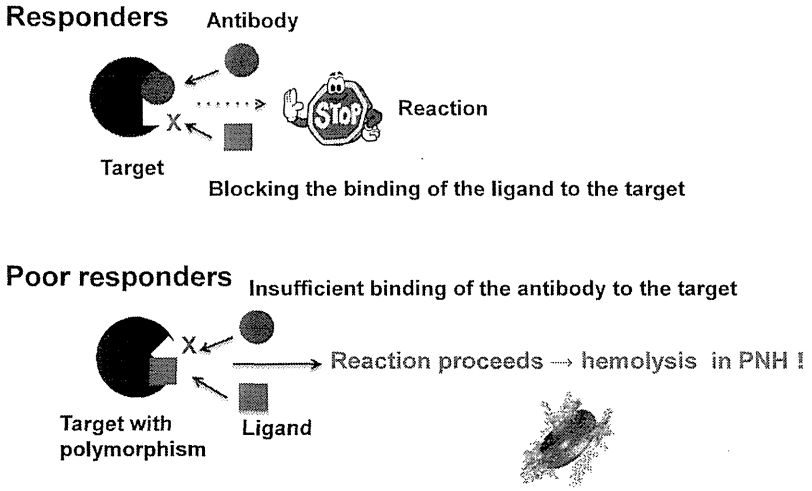

Fig. 5 The mechanism of poor response to antibody therapeutics by genetic polymorphisms of the target molecule.

病状が進行し重篤な状態に曝されている。故に，一日も早い第2世代の治療法の確立が望まれる。

著者のCOI（conflicts of interest）開示：西村純一；講演料（アレクシオンファーマ株式会社），受託研究・共同研究費（アレクシオンファーマ株式会社），奨学寄付金（アレクシオンファーマ株式会社），金倉譲；講演料（アレクシオンファーマ株式会社），受託研究・共同研究費（アレクシオンファーマ株式会社），奨学寄付金（アレクシオンファーマ株式会社）

文　献

1) Hillmen P, Muus P, Röth A, et al. Long-term safety and efficacy of sustained eculizumab treatment in patients with paroxysmal nocturnal haemoglobinuria. Br J Haematol. 2013; **162**: 62-73.
2) Kanakura Y, Ohyashiki K, Shichishima T, et al. Long-term efficacy and safety of eculizumab in Japanese patients with PNH: AEGIS trial. Int J Hematol. 2013; **98**: 406-416.
3) Reiss UM, Schwartz J, Sakamoto KM, et al. Efficacy and safety of eculizumab in children and adolescents with paroxysmal nocturnal hemoglobinuria. Pediatr Blood Cancer. 2014; **61**: 1544-1550.
4) Nishimura J, Yamamoto M, Hayashi S, et al. Genetic variants in C5 and poor response to eculizumab. N Engl J Med. 2014; **370**: 632-639.
5) DeZern AE, Uknis M, Yuan X, et al. Complement blockade with a C1 esterase inhibitor in paroxysmal nocturnal hemoglobinuria. Exp Hematol. 2014; **42**: 857-861.
6) Risitano AM, Ricklin D, Huang Y, et al. Peptide inhibitors of C3 activation as a novel strategy of complement inhibition for the treatment of paroxysmal nocturnal hemoglobinuria. Blood. 2014; **123**: 2094-2101.
7) Nicholson-Weller A, Burge J, Austen KF. Purification from guinea pig erythrocyte stroma of a decay-accelerating factor for the classical C3 convertase, C4b, 2a. J Immunol. 1981; **127**: 2035-2039.
8) Sugita Y, Nakano Y, Tomita M. Isolation from human erythrocytes of a new membrane protein which inhibits the formation of complement transmembrane channels. J Biochem. 1988; **104**: 633-637.
9) Davies A, Simmons DL, Hale G, et al. CD59, an LY-6-like protein expressed in human lymphoid cells, regulates the action of the complement membrane attack complex on homologous cells. J Exp Med. 1989; **170**: 637-654.
10) Rother RP, Bell L, Hillmen P, Gladwin MT. The clinical sequelae of intravascular hemolysis and extracellular plasma hemoglobin: a novel mechanism of human disease. JAMA. 2005; **293**: 1653-1662.
11) Parker C, Omine M, Richards S, et al. International PNH Interest Group. Diagnosis and management of paroxysmal nocturnal hemoglobinuria. Blood. 2005; **106**: 3699-3709.
12) Krawitz PM, Höchsmann B, Murakami Y, et al. A case of paroxysmal nocturnal hemoglobinuria caused by a germline mutation and a somatic mutation in *PIGT*. Blood. 2013; **122**: 1312-1315.
13) Kawagoe K, Kitamura D, Okabe M, et al. Glycosylphosphatidylinositol-anchor-deficient mice: implications for clonal dominance of mutant cells in paroxysmal nocturnal hemoglobinuria. Blood. 1996; **87**: 3600-3606.
14) Rosti V, Tremmi G, Soares V, Pandolfi PP, Luzzatto L, Bessler M. Murine embryonic stem cells without pig-a gene activity are competent for hematopoiesis with the PNH phenotype but not for clonal expansion. J Clin Invest. 1997; **100**: 1028-1036.
15) Murakami Y, Kinoshita T, Maeda Y, Nakano T, Kosaka H, Takeda J. Different roles of glycosylphosphatidylinositol in various hematopoietic cells as revealed by a mouse model of paroxysmal nocturnal hemoglobinuria. Blood. 1999; **94**: 2963-2970.
16) Tremml G, Dominguez C, Rosti V, et al. Increased sensitivity to complement and a decreased red blood cell life span in mice mosaic for a nonfunctional *Piga* gene. Blood. 1999; **94**: 2945-2954.
17) Keller P, Tremml G, Rosti V, Bessler M. X inactivation and somatic cell selection rescue female mice carrying a *Piga*-null mutation. Proc Natl Acad Sci U S A. 1999; **96**: 7479-7483.
18) Wang H, Chuhjo T, Yasue S, Omine M, Nakao S. Clinical significance of a minor population of paroxysmal nocturnal hemoglobinuria-type cells in bone marrow failure syndrome. Blood. 2002; **100**: 3897-3902.
19) Gargiulo L, Lastraioli S, Cerruti G, et al. Highly homologous T-cell receptor beta sequences support a common target for autoreactive T cells in most patients with paroxysmal nocturnal hemoglobinuria. Blood. 2007; **109**: 5036-5042.
20) Gargiulo L, Papaioannou M, Sica M, et al. Glycosylphosphatidylinositol-specific, CD1d-restricted T cells in paroxysmal nocturnal hemoglobinuria. Blood. 2013; **121**: 2753-2761.
21) Araten DJ, Nafa K, Pakdeesuwan K, Luzzatto L. Clonal populations of hematopoietic cells with paroxysmal nocturnal hemoglobinuria genotype and phenotype are present in normal individuals. Proc Natl Acad Sci U S A. 1999; **96**: 5209-5214.
22) Nishimura Ji, Hirota T, Kanakura Y, et al. Long-term support of hematopoiesis by a single stem cell clone in patients with paroxysmal nocturnal hemoglobinuria. Blood. 2002; **99**: 2748-2751.
23) Inoue N, Izui-Sarumaru T, Murakami Y, et al. Molecular basis of clonal expansion of hematopoiesis in 2 patients with paroxysmal nocturnal hemoglobinuria (PNH). Blood. 2006; **108**: 4232-4236.
24) Cavazzana-Calvo M, Payen E, Negre O, et al. Transfusion independence and *HMGA2* activation after gene therapy of human β-thalassaemia. Nature. 2010; **467**: 318-322.

25) Ikeda K, Mason PJ, Bessler M. 3'UTR-truncated Hmga2 cDNA causes MPN-like hematopoiesis by conferring a clonal growth advantage at the level of HSC in mice. Blood. 2011; **117**: 5860-5869.
26) Rother RP, Rollins SA, Mojcik CF, Brodsky RA, Bell L. Discovery and development of the complement inhibitor eculizumab for the treatment of paroxysmal nocturnal hemoglobinuria. Nat Biotechnol. 2007; **25**: 1256-1264.
27) Hillmen P, Hall C, Marsh JC, et al. Effect of eculizumab on hemolysis and transfusion requirements in patients with paroxysmal nocturnal hemoglobinuria. N Engl J Med. 2004; **350**: 552-559.
28) Hill A, Hillmen P, Richards SJ, et al. Sustained response and long-term safety of eculizumab in paroxysmal nocturnal hemoglobinuria. Blood. 2005; **106**: 2559-2565.
29) Hillmen P, Young NS, Schubert J, et al. The complement inhibitor eculizumab in paroxysmal nocturnal hemoglobinuria. N Engl J Med. 2006; **355**: 1233-1243.
30) Brodsky RA, Young NS, Antonioli E, et al. Multicenter phase 3 study of the complement inhibitor eculizumab for the treatment of patients with paroxysmal nocturnal hemoglobinuria. Blood. 2008; **111**: 1840-1847.
31) Kanakura Y, Ohyashiki K, Shichishima T, et al. Safety and efficacy of the terminal complement inhibitor eculizumab in Japanese patients with paroxysmal nocturnal hemoglobinuria: the AEGIS clinical trial. Int J Hematol. 2011; **93**: 36-46.
32) Hillmen P, Muus P, Dührsen U, et al. Effect of the complement inhibitor eculizumab on thromboembolism in patients with paroxysmal nocturnal hemoglobinuria. Blood. 2007; **110**: 4123-4128.
33) Risitano AM, Notaro R, Marando L, et al. Complement fraction 3 binding on erythrocytes as additional mechanism of disease in paroxysmal nocturnal hemoglobinuria patients treated by eculizumab. Blood. 2009; **113**: 4094-4100.
34) Fridkis-Hareli M, Storek M, Mazsaroff I, et al. Design and development of TT30, a novel C3d-targeted C3/C5 convertase inhibitor for treatment of human complement alternative pathway-mediated diseases. Blood. 2011; **118**: 4705-4713.
35) Risitano AM, Notaro R, Pascariello C, et al. The complement receptor 2/factor H fusion protein TT30 protects paroxysmal nocturnal hemoglobinuria erythrocytes from complement-mediated hemolysis and C3 fragment. Blood. 2012; **119**: 6307-6316.

The C5 gene polymorphism in patients with PNH

Jun-ichi NISHIMURA, Yuzuru KANAKURA

Osaka University Graduate School of Medicine, Department of Hematology and Oncology

Key words : Paroxysmal nocturnal hemoglobinuria, Complement mediated intravascular hemolysis, Eculizumab, Gene polymorphism

This review is a commentary on an article entitled "Genetic variants in C5 and poor response to eculizumab" (N Engl J Med. 2014; 370: 632-639). The molecular basis for the poor response to eculizumab in Japanese patients is unclear. Of 345 Japanese patients with paroxysmal nocturnal hemoglobinuria (PNH) who received eculizumab, 11 showed a poor response. All 11 had a single missense C5 heterozygous mutation, c.2654 G>A, which predicts the polymorphism p.Arg885His. The prevalence of this mutation among patients with PNH (3.2%) was similar to that in healthy Japanese persons (3.5%). This polymorphism was also identified in a Han Chinese population. Non-mutant and mutant C5 both caused hemolysis *in vitro*, but only non-mutant C5 bound to and was blocked by eculizumab. *In vitro* hemolysis due to non-mutant and mutant C5 was completely blocked by N19-8, a monoclonal antibody that binds to a different site on C5 than does eculizumab. The functional capacity of the C5 polymorphism p.Arg885His, together with its failure to undergo blockade by eculizumab, accounts for the poor response to this agent in patients who carry this mutation.

European Journal of Immunology

Estrogen-inducible sFRP5 inhibits early B-lymphopoiesis in vivo, but not during pregnancy

Takafumi Yokota[1], Kenji Oritani[1], Takao Sudo[1], Tomohiko Ishibashi[1], Yukiko Doi[1], Yoko Habuchi[1], Michiko Ichii[1], Kentaro Fukushima[1], Daisuke Okuzaki[2], Kazuma Tomizuka[3], Kengo Yamawaki[4], Makoto Kakitani[5], Akihiko Shimono[6], Eiichi Morii[7], Paul W. Kincade[8] and Yuzuru Kanakura[1]

[1] Department of Hematology and Oncology, Osaka University Graduate School of Medicine, Suita, Osaka, Japan
[2] DNA-chip Development Center for Infectious Diseases, Research Institute for Microbial Diseases, Osaka University, Suita, Osaka, Japan
[3] Kyowa Hakko Kirin California, Inc. Research Divisions, CA, USA
[4] Kyowa Hakko Kirin Co., Ltd. Biologics Research Laboratories, Research Division, Machida, Tokyo, Japan
[5] Kyowa Hakko Kirin Co., Ltd. Bio Process Research and Development Laboratories, Takasaki, Gunma, Japan
[6] TransGenic Inc. 7-1-14 Minatojima-minami, Chuo, Kobe, Japan
[7] Department of Pathology, Osaka University Graduate School of Medicine, Osaka, Japan
[8] Immunobiology and Cancer Program, Oklahoma Medical Research Foundation, Oklahoma City, OK, USA

Mammals have evolved to protect their offspring during early fetal development. Elaborated mechanisms induce tolerance in the maternal immune system for the fetus. Female hormones, mainly estrogen, play a role in suppressing maternal lymphopoiesis. However, the molecular mechanisms involved in the maternal immune tolerance are largely unknown. Here, we show that estrogen-induced soluble Frizzled-related proteins (sFRPs), and particularly sFRP5, suppress B-lymphopoiesis in vivo in transgenic mice. Mice overexpressing sFRP5 had fewer B-lymphocytes in the peripheral blood and spleen. High levels of sFRP5 inhibited early B-cell differentiation in the bone marrow (BM), resulting in the accumulation of cells with a common lymphoid progenitor (CLP) phenotype. Conversely, sFRP5 deficiency reduced the number of hematopoietic stem cells (HSCs) and primitive lymphoid progenitors in the BM, particularly when estrogen was administered. Furthermore, a significant reduction in CLPs and B-lineage-committed progenitors was observed in the BM of *sfrp5*-null pregnant females. We concluded that, although high sFRP5 expression inhibits B-lymphopoiesis in vivo, physiologically, it contributes to the preservation of very primitive lymphopoietic progenitors, including HSCs, under high estrogen levels. Thus, sFRP5 regulates early lympho-hematopoiesis in the maternal BM, but the maternal–fetal immune tolerance still involves other molecular mechanisms that remain to be uncovered.

Keywords: B-lymphopoiesis · Bone marrow · Estrogen · Hematopoietic stem cells · Immune tolerance · Lymphoid progenitors · Pregnancy · Soluble Frizzled-related proteins

Additional supporting information may be found in the online version of this article at the publisher's web-site

Correspondence: Dr. Takafumi Yokota
e-mail: yokotat@bldon.med.osaka-u.ac.jp

© 2015 WILEY-VCH Verlag GmbH & Co. KGaA, Weinheim

Introduction

Adult lymphopoiesis is dramatically suppressed during pregnancy. However, its physiological significance and underlying mechanisms have remained elusive [1, 2]. Our previous studies demonstrated that gonadal hormones, particularly estrogen, play pivotal roles in suppressing maternal B-cell lymphopoiesis [3–6]. In the present study, our primary goal was to identify molecules that participate in this process.

Global analyses of estrogen-inducible genes in bone marrow (BM) stromal cells have led to the identification of members of the secreted Frizzled-related protein (sFRP) family [7]. The five mammalian sFRPs are agonists or antagonists of the canonical Wingless and Int-1 (Wnt) signaling pathway [8, 9]. We previously showed that sFRP1 expression in hematopoiesis-supporting stromal cell lines correlated with their inability to promote lymphopoiesis [7], and the recombinant sFRP1-fusion protein selectively blocked lymphocyte formation in culture. Furthermore, sFRP1 levels were elevated in response to estrogen treatment. Thus, it was proposed that sFRP1 might function within the BM to control the number of new lymphocytes that are produced during both the steady state and pregnancy. In support of this idea, the elimination of the *sFRP1* gene was shown to elevate B-cell numbers in the BM and blood [10]. The quality of hematopoietic stem cells (HSCs) was also affected, indicating additional roles for sFRPs.

SFRPs contain a cysteine-rich domain (CRD) in the N-terminal region, which shares homology with the CRD of "Frizzled" receptors and serves as a binding surface for Wnt proteins [8, 11]. Wnt proteins play vital roles in various biological activities, including development and immune system function [12, 13]. Because the Frizzled receptors initiate Wnt signal transduction in both canonical and noncanonical pathways, sFRPs that modulate the association between Wnt and Frizzled receptors are presumed to have biological importance. However, sFRP1 and the other four members of the sFRP family have remained unstudied with respect to their roles in the regulation of lymphopoiesis during pregnancy. Herein, we report that sFRP5 expression is strongly upregulated by estrogen and preferentially influences B-cell progenitors in vivo. SFRP5 is a potent regulator of maternal lympho-hematopoiesis, but not as we originally hypothesized.

Results

Overexpression of sFRP1 and sFRP5 in vivo reduces B-lineage cells

We previously performed global analyses of estrogen-inducible genes in BM stromal cells and identified the sFRP family [7]. Estrogen treatment markedly upregulated the expression of sFRP1 in BM stromal cells, and a sFRP1-immunoglobulin (Ig)-fusion protein inhibited differentiation of B-lineage cells that originated from BM-derived hematopoietic stem/progenitor cells in culture [7]. Conversely, sFRP1 deficiency in vivo causes dysregulation of HSC homeostasis in BM and aberrant increase of peripheral B-lymphocytes [10]. Therefore, we generated sFRP1-transgenic (TG) mice that produced high levels of circulating sFRP1 in vivo.

Since induced expression of sFRPs is known to disturb normal embryonic development [14], we designed a TG system in which sFRP1 was overexpressed after birth so that we could specifically examine the influence of sFRP1 on adult lymphopoiesis (Fig. 1A) [15]. Furthermore, we generated sFRP5-TG mice using the same procedure to determine whether there were functional differences or redundancies between sFRP1 and sFRP5, which are the two most closely related isoforms in the sFRP family (Fig. 1B) and are known to play similar roles during embryonic development [16]; however, their physiological function in the adult immune system is largely unknown. Our initial experiments indicated that both *sFRP1* and *sFRP5* genes were highly responsive to estrogen exposure in adult murine BM (Fig. 1C).

The number of B-lymphocytes, identified by the expression of CD45R/B220 and/or CD19, was significantly reduced in the spleen but not in the peripheral blood of sFRP1-TG mice when examined at 10 weeks of age (Fig. 2A–C). Unexpectedly, a more dramatic reduction of B-lineage cells was found in sFRP5-TG mice, even in the peripheral blood. The frequency of $B220^+$ B cells, which typically account for approximately 50% of peripheral leukocytes of WT mice, was reduced to less than 20% in the sFRP5-TG mice, whereas the absolute numbers of myeloid, erythroid, T-lineage lymphoid, and NK cells remained unaffected (Fig. 2D). Notably, the magnitude of this suppressive effect on B-lineage cells differed among individuals and in a subgroup of the sFRP5-TG mice that exhibited severe B-lymphocytopenia (Fig. 2E).

We further analyzed the phenotypes of the sFRP1-or sFRP5-TG mice. Both strains were fertile and thrived. The body size of sFRP1-TG mice did not significantly change compared with their WT littermates (data not shown); however, sFRP5-TG mice were slightly but significantly smaller (Fig. 3A). The total number of spleen cells was reduced twofold and the organs themselves appeared small in sFRP5-TG mice (Fig. 3A–B), while the total number of thymus cells was slightly but not significantly decreased (Fig. 3A). The white pulp of WT spleens contained lymphoid follicles with a few germinal centers, but germinal centers were obliterated in the follicles of the sFRP5-TG spleens (Fig. 3B, right panel). Instead, the white pulp of sFRP5-TG spleens developed marginal and perifollicular zones. Consistent with the structural changes in the spleen, the ratios between T- and B-lineage cells were unbalanced (Fig. 3C, left panel). Although the T-cell population exhibited a compensatory increase in terms of percentage, the absolute numbers were slightly lower than those in the WT controls (Fig. 3C, right panel). Furthermore, the absolute numbers of B-lineage cells dramatically decreased in the spleens of sFRP5-TG mice (Fig. 3C, right panel).

Splenic B-cell lineage cells can be fractionated into subcategories according to the expression patterns of cell surface antigens. AA4.1 marks newly formed cells migrating from the BM to the spleen, and these cells can be further divided into transitional 1–3 (T1–T3) fractions according to the expression of IgM and CD23 [17]. The $AA4.1^+$ population was significantly reduced

© 2015 WILEY-VCH Verlag GmbH & Co. KGaA, Weinheim

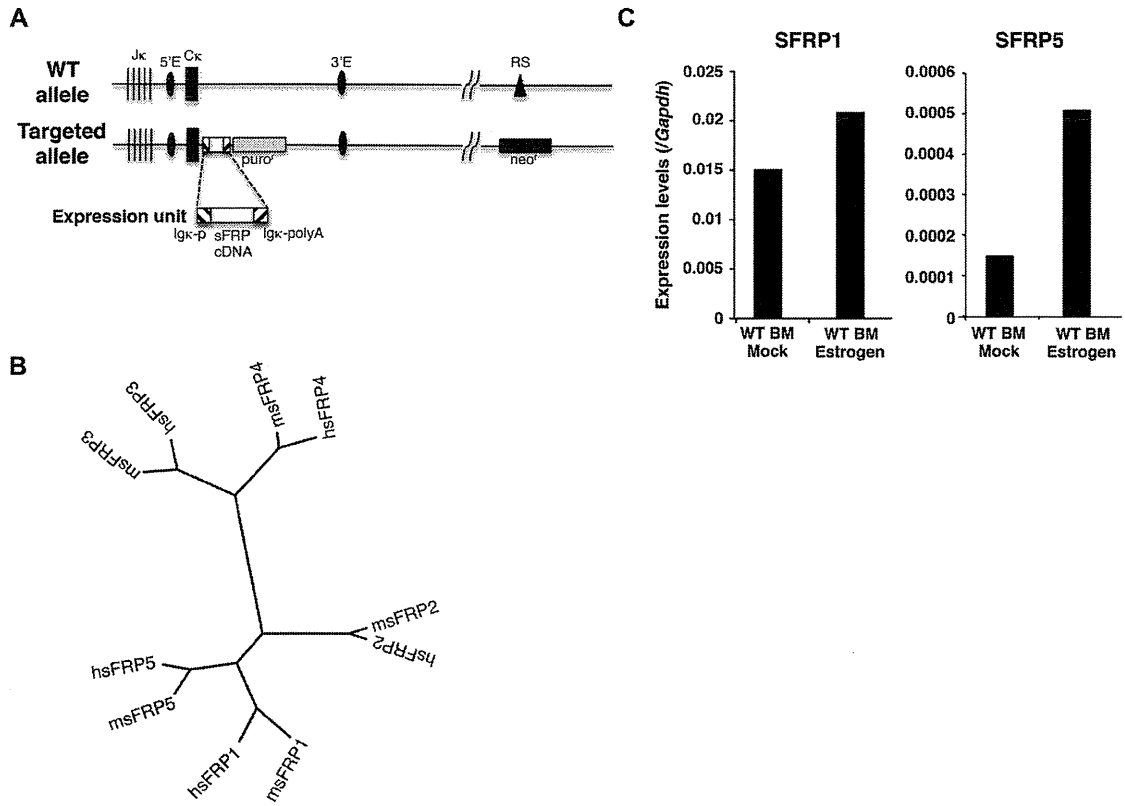

Figure 1. Generation of sFRP-TG mice and comparison of sFRP1 and sFRP5. (A) Transgenic strategy targeting the endogenous *Igκ* locus. (Upper) WT endogenous *Igκ* locus: 5′ E, *Igκ* intronic enhancer; 30′E, *Igk* 3′-enhancer; RS, recombining sequence. (Lower) Targeting construct. The transcriptional unit that consists of the *Igκ*-promoter, sFRP cDNA, and *Igκ*-poly(A) signal is flanked downstream by a puromycin-resistance (puro^r) gene. The construct was inserted downstream of the Cκ exon. The recombining sequence (RS) of WT mice was replaced by a G418-resistance (neo^r) cassette in the targeting allele. (B) Phylogenetic tree based on the coding sequences of members of the mouse and human sFRP families was generated using the neighbor-joining method. (C) Quantitative real-time PCR analyses were performed to evaluate the levels of sFRP1 and sFRP5 expression in BM before and after estrogen treatment. Data are representative of two independent experiments, with $n = 3$ samples/group.

in the spleens of sFRP5-TG mice (Fig. 3D, left panels), and the newly immigrated T1 fraction was the most affected (Fig. 3D, middle panels). In contrast, the proportion and absolute number of AA4.1$^-$ cells were affected to a lesser degree. Among the AA4.1$^-$ fraction, cells possessing the IgM^{hi} IgD$^{-/lo}$ marginal-zone phenotype were proportionally preserved (Fig. 3D, right panels). Similar to the marginal-zone B cells, B1-B cells, characterized by CD5 expression, participate in innate immunity by rapidly responding to antigenic challenges in a T cell-independent manner [18]. Interestingly, we found that cells with the B1-B characteristics were comparatively retained even in the spleen of sFRP5-TG mice from which B-lineage cells were almost depleted (Fig. 3E).

Overexpression of sFRP5 blocks a distinct early stage in B-lymphopoiesis

We then chose to focus our efforts on lympho-hematopoiesis in the sFRP5-TG mice because they exhibited more remarkable phenotypes than those of the sFRP1-TG mice. Because the numbers of newly formed B cells were reduced in the spleens of sFRP5-TG mice, we consequently examined BM, where mammalian B-lineage cells develop throughout life from HSCs through progressive stages of differentiation (Fig. 4A) [19].

We observed a dramatic reduction in CD43^{lo} B220$^+$ AA4.1$^+$ surface IgM$^-$ PreB and CD43$^-$ B220^{hi} AA4.1$^+$ surface IgM$^+$ immature B cells in sFRP5-TG mice (Fig. 4B–C). While the total number of BM mononuclear cells was slightly decreased in sFRP5-TG mice probably because of the reduction of body size, the reduction in B-lineage precursors was more significant (Fig. 4C). We also observed that IL-7-responsive lymphoid progenitors decreased in sFRP5-TG mice, whereas myeloid/erythroid progenitors proportionately increased in clonal assays (Fig. 4D).

The expression of c-kit, a stem cell factor receptor, and the absence of lineage-related markers (Lin) define primitive hematopoietic progenitors. The frequency of these Lin$^-$ c-kit$^+$ progenitor cells significantly increased in the BM of sFRP5-TG mice (Fig. 4E). We also observed an approximate 1.2-fold increase in the fraction of Lin$^-$ Sca1$^-$ c-kit^{hi} myeloid progenitors. The frequency and absolute numbers of the HSC-enriched Lin$^-$ Sca-1$^+$ c-kit^{hi} (LSK) Flt3$^-$ fraction remained unaffected, and the same was true for the LSK Flt3$^+$ fraction, including multilineage progenitors

© 2015 WILEY-VCH Verlag GmbH & Co. KGaA, Weinheim

A

	WT	SFRP1-TG	P value
WBC (/μl)	4920 ± 440	4470 ± 380	NS
Mac1$^+$ (%)	9.7 ± 1.0	13.5 ± 1.0	<0.01
B220$^+$ (%)	50.6 ± 2.2	47.4 ± 1.2	NS
CD3$^+$ (%)	29.6 ± 1.8	31.2 ± 1.1	NS
NK1.1$^+$ (%)	6.1 ± 0.6	6.4 ± 0.4	NS
Mac1$^+$(/μl)	490 ± 80	600 ± 60	NS
B220$^+$(/μl)	2480 ± 230	2120 ± 190	NS
CD3$^+$ (/μl)	1470 ± 180	1320 ± 90	NS
NK1.1$^+$ (/μl)	310 ± 50	280 ± 10	NS
RBC (x10^4/μl)	896 ± 13	879 ± 17	NS
Hb (g/dl)	13.7 ± 0.3	13.2 ± 0.3	NS
HCT(%)	54.1 ± 0.2	54.2 ± 0.2	NS
MCV(fL)	54.1 ± 0.2	54.2 ± 0.2	NS
MCH(pg)	15.3 ± 0.1	15.1 ± 0.1	NS
MCHC(g/dL)	28.2± 0.2	27.8 ± 0.2	NS
Plt (x10^4/μl)	99.8 ± 3.1	88.9 ± 3.4	<0.05

B

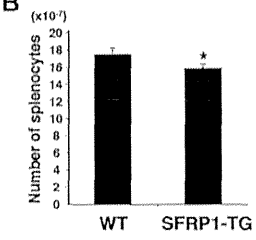

C

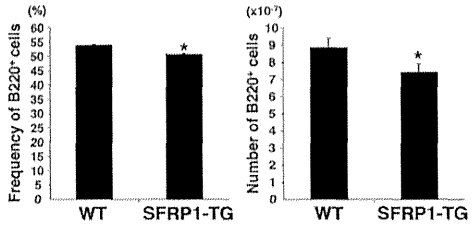

D

	WT	SFRP5 -TG	p value
WBC (/μl)	4200 ± 550	2200 ± 170	< 0.01
Mac1$^+$ (%)	16.0 ± 1.6	28.4 ± 3.2	< 0.01
B220$^+$ (%)	56.3 ± 2.3	15.6 ± 3.6	< 0.001
CD3$^+$ (%)	27.0 ± 2.5	51.1 ± 3.3	< 0.01
NK1.1$^+$ (%)	9.2 ± 0.8	14.9 ± 1.9	< 0.05
Mac1$^+$(/μl)	640 ± 90	610 ± 70	NS
B220$^+$(/μl)	2460 ± 400	370 ± 90	< 0.001
CD3$^+$ (/μl)	1100 ± 140	1100 ± 100	NS
NK1.1$^+$ (/μl)	290 ± 10	330 ± 60	NS
RBC (x10^4/μl)	773 ± 21	828 ± 60	NS
Hb (g/dl)	11.7 ± 0.4	12.1 ± 1.0	NS
Ht (%)	43.0 ± 1.9	43.9 ± 3.8	NS
MCV(fL)	55.4 ± 1.0	53.1 ± 0.9	< 0.01
MCH(pg)	15.1 ± 0.2	14.7 ± 0.3	< 0.01
MCHC(g/dL)	27.3± 0.5	27.6 ± 0.4	NS
Plt (x10^4/μl)	103.0 ± 10.0	90.5 ± 15.4	NS

E

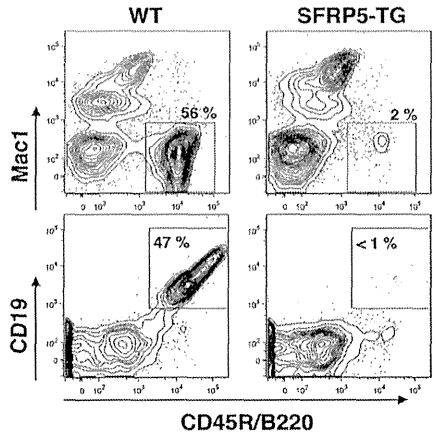

Figure 2. Overexpression of sFRP reduces the number of peripheral B-lymphocytes. (A) Peripheral blood samples from 10-week-old sFRP1-TG heterozygous females ($n = 7$) and their WT littermates ($n = 10$) were analyzed. White blood cells (WBCs), red blood cells (RBCs), hemoglobin (Hb), hematocrit (Ht), mean corpuscular volume (MCV), mean corpuscular hemoglobin (MCH), mean corpuscular hemoglobin concentration (MCHC), and platelets (Plt) were counted using a blood cell analyzer (Sysmex KX-21). The proportion of Mac1$^+$ myeloid, B220$^+$ B, CD3$^+$ T, and NK1.1$^+$ NK cells was determined using flow cytometry for each individual mouse. Absolute cell numbers were calculated by multiplying WBC counts by their percentages. Data are shown as mean ± SEM and are pooled from three independent experiments. (B) Total splenocyte counts of the sFRP1-TG heterozygous females and their WT littermates are shown. (C) The proportion of B220$^+$ B cells of the TER119$^-$ fraction was determined by FACS. The absolute numbers were calculated by multiplying splenocyte counts by the percentages of B220$^+$ cells. Data are shown as mean + SEM and are pooled from three independent experiments (*$p < 0.05$, unpaired two-tailed t-tests). (D) Peripheral blood data of 5~7-week-old sFRP5-TG heterozygous females ($n = 9$) and their WT littermates ($n = 9$) are shown. Data are shown as mean ± SEM and are pooled from three littermate pairs. The proportion of each lineage was determined using the same method applied to sFRP1-TG mice as described in (A). (E) Representative profiles of severe B lymphocytopenia observed in peripheral WBCs of sFRP5-TG (right) and their WT littermates (left). Cells were stained with antibodies against Mac1, B220, and CD19. The percentage of the gated fraction of the total number of WBCs is shown in each panel. Plots are representative of three independent experiments.

(MLPs) and early lymphoid progenitors (ELPs) (Fig. 4F). By mating Rag1/GFP reporter mice to sFRP5-TG mice, we also demonstrated that sFRP5 overexpression did not affect Rag1/GFP$^+$ ELPs (Fig. 4G).

Notably, among the Lin$^-$ c-Kit$^+$ cells, we detected a significant increase of the Lin$^-$ c-kit^{lo} Sca1$^{-/Lo}$ Flt3$^+$ IL7Rα$^+$ fraction, which was originally described as common lymphoid progenitors (CLPs) [20], in the BM of sFRP5-TG mice (Fig. 4H). These results suggest that high levels of sFRP5 block the differentiation of the B-lineage cells between CLPs and Pro/PreB cells, but spare the more primitive hematopoietic cells and mildly skew their differentiation potential in the direction of myeloid lineage cells. When CLPs were harvested from the transgenic mice, washed, and placed in culture, they were found to normally differentiate to generate

© 2015 WILEY-VCH Verlag GmbH & Co. KGaA, Weinheim

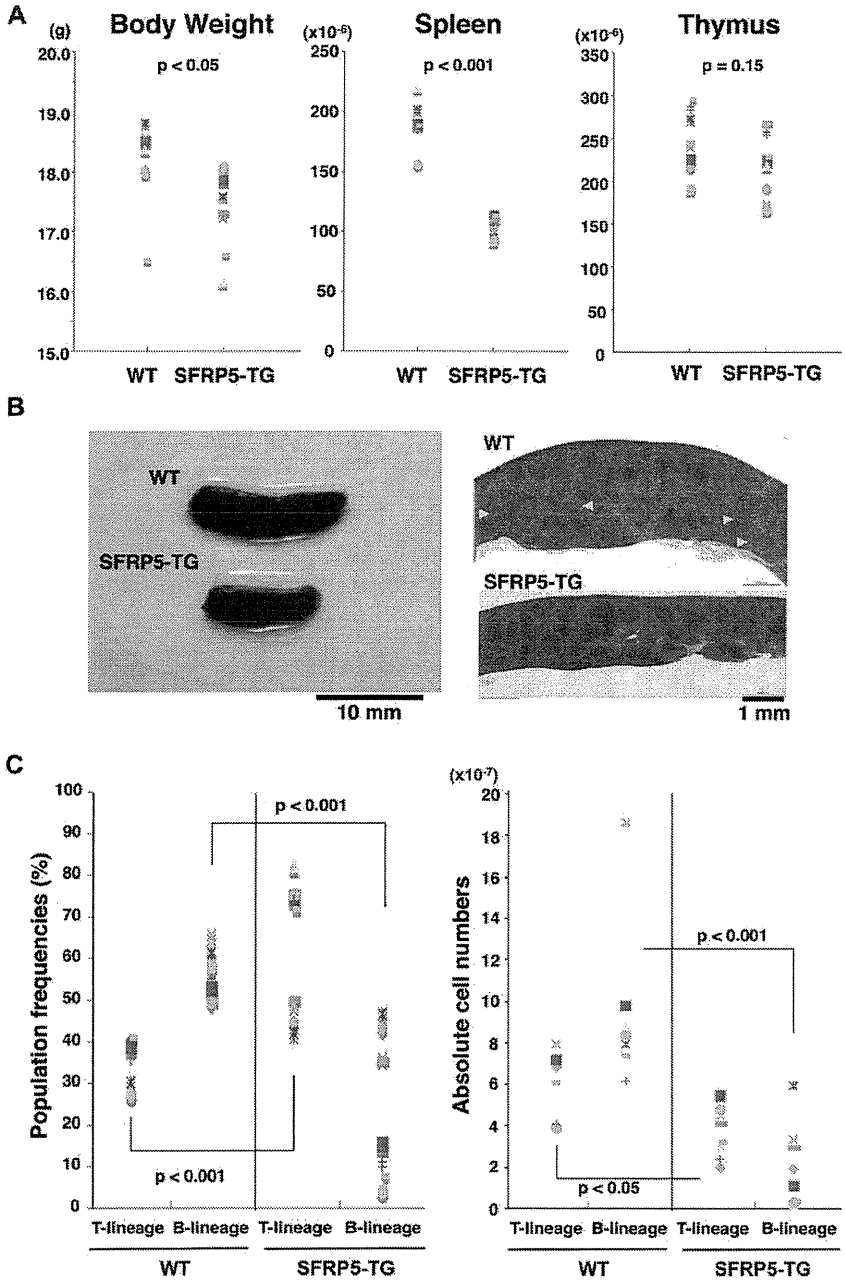

Figure 3. Phenotypes of sFRP5-TG mice (A), body weight and cell numbers in the spleen and thymus are shown and compared between sFRP5-TG heterozygous females (n = 9) and their WT littermates (n = 8) at the age of 0~1 day and 7 weeks. Data are pooled from three littermate pairs. Significant differences are shown in each panel as the p value. (B) (Left) SFRP5-TG spleens are smaller than those of the WT littermates. (Right) H&E-stained sections were examined under 40× magnification. Yellow arrowheads indicate germinal centers in white pulps of the spleen sections, which were identified microscopically as areas that stain less intensely due to the presence of fewer cells and apoptotic B-cells. Images are representative of three independent experiments. (C) The frequency of T- and B-lineage cells in the spleen was determined by FACS. Splenocytes from 5~6-week-old sFRP-TG mice and their WT littermates were stained with antibodies against CD3, B220, CD19, Mac1, and Ter119 antibodies. Frequencies of T-lineage ($CD3^+$ $B220^-$ $CD19^-$ $Mac1^-$ $Ter119^-$) and B-lineage ($CD3^-$ $B220^+$ $CD19^+$ $Mac1^-$ $Ter119^-$) cells among $Ter119^-$ cells are shown in the left panel. The absolute numbers of T- and B-lineage cells were calculated by multiplying splenocyte counts by their frequencies and shown in the right panel. Data are pooled from three littermate pairs. (D) Splenocytes were fractionated according to the expression of surface antigens into transitional 1–3 (T1–T3), marginal zone (MZ), follicular (FL) I, and FL II + marginal zone progenitors (MZPs). (E) Splenocytes were stained with antibodies against CD5, CD19, Mac1, and Ter119, and the frequencies of $CD5^+$ $CD19^+$ B1-B cells and $CD5^-$ $CD19^+$ B2-B cells among $Ter119^-$ cells were evaluated. The percentage of cells in their respective parental fractions is shown in each panel. (D and E) Plots are representative of three independent experiments.

B-lineage lymphocytes (Fig. 4I). These findings enable us to infer the arrested stage and indicate that differentiation is no longer blocked when sFRP5 is removed.

SFRP5 deficiency has no obvious impact on peripheral B-lymphocytes

Considering the elevated number of B-lymphocytes in sFRP1-knockout (KO) mice [10] and the potent B-lineage suppression observed in the sFRP5-TG mice, we expected to see increased B-lymphocyte formation in sFRP5-deficient animals. Surprisingly, however, $B220^+$ cells in the peripheral blood of sFRP5-KO mice were found to be within the normal range (49.9 ± 3.4%; n = 8). Furthermore, no remarkable differences were observed in spleen sizes or BM $B220^+$ cell counts between WT and sFRP5-KO mice.

These findings called into question the influence of sFRP5 in normal, steady-state B-lymphopoiesis, and we wondered if the differences observed between sFRP1 and sFRP5 were related to their constitutive levels. Previous studies demonstrated that sFRP1 is a product of osteoblasts and can be detected using immunohistochemical staining or real-time RT-PCR [7, 21]. Indeed, while sFRP1 was abundantly expressed in steady-state BM and only slightly upregulated by our TG system, sFRP5 levels in normal

© 2015 WILEY-VCH Verlag GmbH & Co. KGaA, Weinheim

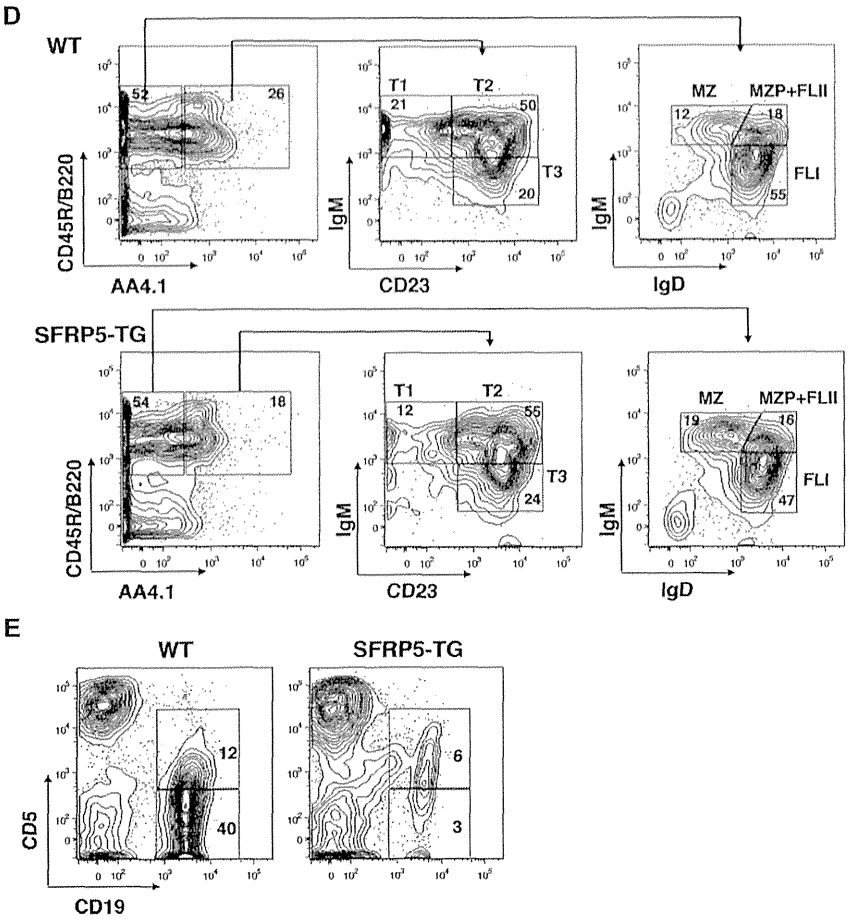

Figure 3. Continued

BM were very low, but significantly upregulated in the TG mice (Supporting Information Fig. 1). In addition, transcript levels of *sFRP5* in vivo were found to be approximately 100-fold lower than those of *sFRP1* (Supporting Information Fig. 2). As shown above, sFRP5 was markedly induced when mice were injected with β-estradiol (Fig. 1C). Thus, these two proteins may have overlapping functions but may become functionally dissimilar under different circumstances in vivo.

SFRP5 deficiency influences early B-lymphopoiesis under elevated estrogen conditions

The above results suggest that the physiological expression of sFRP5, particularly when induced by high levels of estrogen, could influence the production of immune cells. To test this hypothesis, we injected water-soluble β-estradiol into WT or sFRP5-KO mice at 1 mg/day for 4 days and evaluated early lymphoid differentiation in BM 12 h after the last injection. Continuous and lengthy treatment with estrogen causes hypermineralized bone with small BM cavities, resulting in a decreased number of BM cells, including lymphoid progenitors [3]. However, the 4-day estrogen treatment performed in this study did not significantly affect the number of BM cells (BM cell counts in 1 femur + 1 tibia: WT treated with saline alone, $37.4 \pm 1.1 \times 10^6$; WT treated with β-estradiol, $35.5 \pm 0.9 \times 10^6$; sFRP5-KO treated with saline alone, $36.6 \pm 0.8 \times 10^6$; and sFRP5-KO treated with β-estradiol, $33.3 \pm 1.5 \times 10^6$; $n = 7$ for each group).

While the HSC-enriched LSK $Flt3^-$ cells of WT mice decreased after short-term estrogen treatment, the corresponding fraction in sFRP5-KO mice was more significantly suppressed (Fig. 5A). Although the MLP-, ELP-, and CLP-enriched fractions were drastically reduced in both strains, the lymphoid progenitors of sFRP5-KO mice were unexpectedly more sensitive to estrogen than those of WT (Fig. 5A). We also evaluated the numbers of ProB, PreB, and immature B cells in WT and sFRP5-KO mice after estrogen treatment and found that those B-cell precursors were not significantly affected in sFRP5-KO mice (Fig. 5B). Thus, we concluded that estrogen-induced sFRP5 counteracts the negative effect of estrogen at the very early stage of lymphopoiesis when hematopoietic stem/progenitor cells initiate differentiation toward the B-lymphoid lineage.

To explore the physiological roles of sFRP5 in lymphopoiesis during pregnancy, we evaluated the proportion and absolute number of B-lineage progenitors in pregnant sFRP5-KO mice. To avoid the possible influence of fetal-produced sFRP5 on maternal lymphopoiesis, we mated WT females with WT males and sFRP5-KO

© 2015 WILEY-VCH Verlag GmbH & Co. KGaA, Weinheim

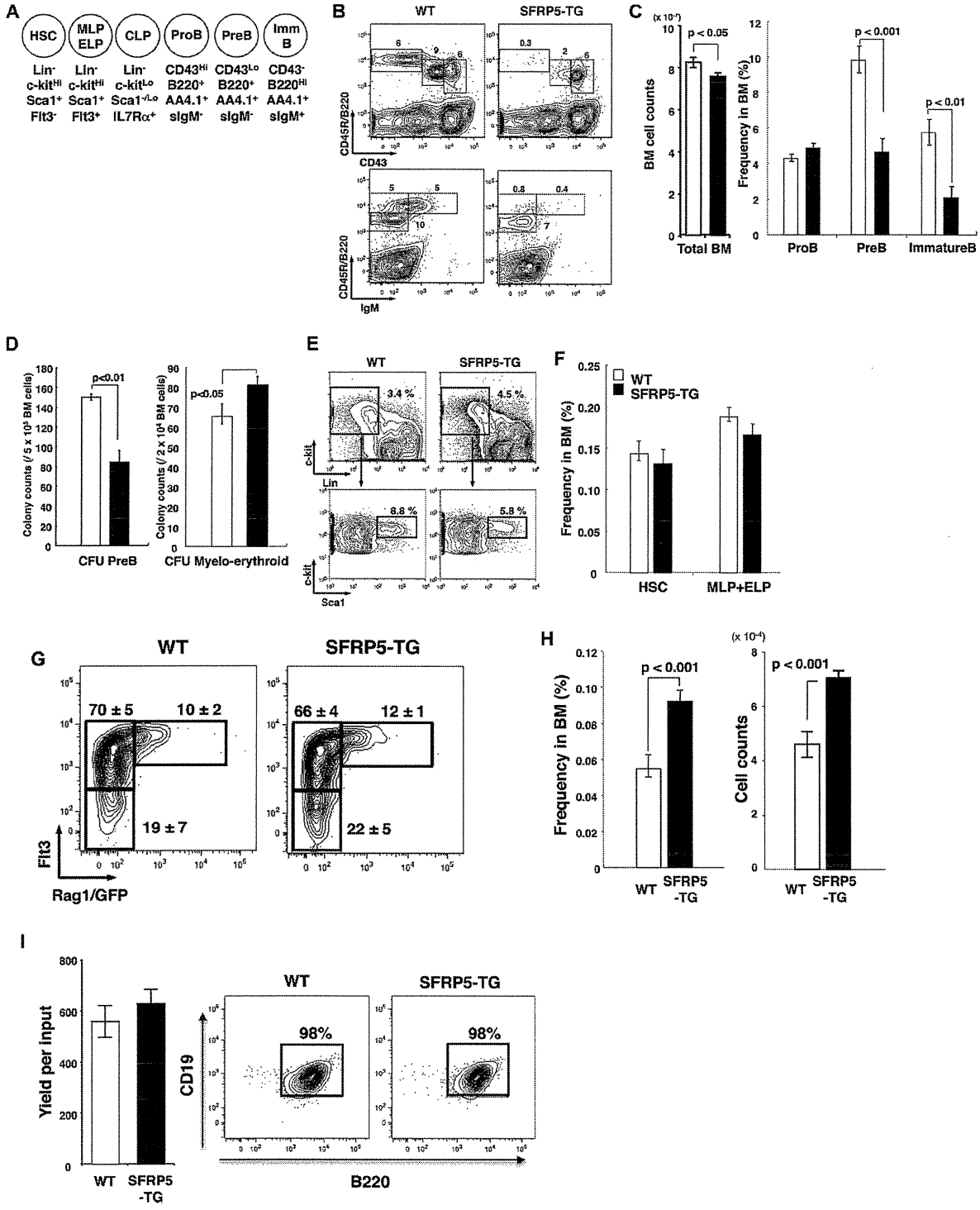

Figure 4. Early stages of B-lymphocyte differentiation are sustained in sFRP5-TG mice. (A) Schematic of B-lymphocyte differentiation in BM. B-lineage cells generated from HSCs are characterized by the rearrangement of immunoglobulin genes, resulting in the expression of surface IgM (sIgM)-positive immature B cells (Imm B). The phenotypes of each stage are shown below. (B) The cells in the $B220^{+}$ $CD43^{lo}$ $sIgM^{-}$ PreB and $B220^{hi}$ $CD43^{-}$ $sIgM^{+}$ immature B fractions were significantly reduced in the BM of sFRP5-TG mice. FACS profiles for 7-week-old female sFRP5-TG (right) or WT littermates (left) are representative of three independent experiments. (C) Absolute numbers of BM cells of the sFRP5-TG mice (black) and their WT littermates (white) are shown in the left panel. BM cells were collected from two femurs and two tibias. Frequencies of pro-B, pre-B, and immature B cells were calculated ($n = 7$ for each genotype) and are shown in the right panel. (D) Data acquired using methylcellulose colony assays (left, CFU-IL7; right, CFU-myeloid and/or erythroid) are shown (WT, white; SFRP5-TG, black). (E).The frequencies of Lin^{-} c-Kit^{+} cells among BM cells are shown in upper panels. The frequencies of LSK cells among the Lin^{-} c-Kit^{+} fraction are shown in lower panels. Plots are representative

© 2015 WILEY-VCH Verlag GmbH & Co. KGaA, Weinheim

females with sFRP5-KO males. Pregnant females of both strains were analyzed on gestation day 17.5. We found that the frequencies and absolute numbers of cells in the HSC and MLP + ELP fractions were markedly increased by pregnancy in both strains (Fig. 5C).

Although no apparent differences were detected between WT and sFRP5-KO pregnant mice with respect to the HSC or MLP and ELP fractions, the proportion and absolute number of CLPs in pregnant sFRP5-KO mice were significantly lower than those in pregnant WT mice and nonpregnant sFRP5-KO mice (Fig. 5C). On the other hand, the frequencies and absolute numbers of ProB, PreB, and immature B cells were dramatically decreased by pregnancy in WT mice, but the decrease was not significantly changed in sFRP5-KO mice (Fig. 5D). It is noteworthy that in the absence of sFRP5 during pregnancy, the level of expression of the other four sFRPs was increased in the BM (Supporting Information Fig. 3). These results suggest that, although estrogen-inducible sFRP5 might play some roles in early B-lymphopoiesis during pregnancy, other unknown mechanisms are still involved in the suppression of maternal B-lymphopoiesis.

Discussion

The adaptive immune system is not replenished during pregnancy; however, how and why this happens is still unclear. Although elevated sex steroids are partly responsible for this phenomenon, multiple cell types, and hormone-regulated proteins also appear to be involved. Here, we teased out and compared two associated proteins, sFRP1 and sFRP5, by manipulating their levels using transgenic animals and gene targeting. While both sFRP1 and sFRP5 are elevated under high estrogen conditions and can suppress B-lymphopoiesis, these structurally related proteins have discrete roles and do not account for all pregnancy-related changes. Our results provide novel insights into the functional differences between the sFRP family members in vivo and underscore the importance of the complexities associated with pregnancy.

Our previous study identified sFRP1 as an estrogen-inducible gene in BM stromal cells [7]. While we observed that the levels of sFRP1 in stromal cells correspond to their inability to support B-cell differentiation, an alternate study demonstrated that high sFRP1 expression correlates with the ability to maintain HSCs [10]. Furthermore, both studies suggested that sFRP1 is necessary to stabilize the canonical Wnt signaling pathway, which is important for stem cell integrity [22]. Based on these findings, we inferred that sFRP1 is important for maintaining the quality of HSCs by inhibiting their differentiation. Thus, we speculated that sFRP1 overexpression would increase HSCs by inhibiting their differentiation to B-lymphocytes.

Surprisingly, sFRP5 overexpression caused a much greater reduction in the number of B-lymphocytes in vivo than sFRP1. On the other hand, gene targeting of sFRP1 but not sFRP5 in otherwise normal animals increased the peripheral B-cell number. These contradictory results may be attributed to several factors. It is possible that the observed difference is caused by the substantially different physiological amounts of sFRP1 and sFRP5, as shown in this study. While sFRP1 is, to some degree, constitutively produced, sFRP5 is more likely to be an inducible protein. Physiological amounts of sFRP5 under homeostatic conditions may be lower than the functional threshold required to suppress B-lymphopoiesis.

Alternatively, it is possible that sFRP5 functionally differs from sFRP1 in regulating lymphopoiesis. Indeed, while changes at the stem cell and myeloid progenitor levels were recorded in sFRP1-KO mice, sFRP5 appeared to be primarily involved at a later, committed stage of lymphoid differentiation. CLPs are not only spared but they also accumulate in sFRP5-overexpressing mice. Moreover, in contrast to the sFRP1-TG mice, sFRP5 overexpression severely deprived the peripheral blood of B-lineage populations. Thus, although both sFRP1 and sFRP5 act as negative regulators for B-lymphopoiesis, there are substantial differences between the two with respect to their target cells and biological activities.

Wnt signaling has been linked to self-renewal and integrity of HSCs and progenitors, and a delicate balance seems to exist in Wnt signaling based on the physiological demand [23, 24]. It is possible that sFRP1 and sFRP5 modify the same Wnt signaling pathway in different ways to regulate hematopoietic cell differentiation. Early studies identified sFRPs as Wnt antagonists since they bind to Wnts via the Frizzled receptor-like CRD [25–27]. However, accumulating evidence suggests that sFRPs are not merely Wnt antagonists but have a wider range of biological functions than previously expected [14, 28–31].

In the case of Wnt signaling regulation, sFRPs can serve as agonists or antagonists depending on the context, concentration, and expression pattern of Frizzled receptors in target cells [32]. Because the CRD of sFRPs can directly interact with the CRD of

of three independent experiments with 7-week-old female littermates. (F) The frequencies of the LSK Flt3$^-$ HSC-enriched or LSK Flt3$^+$ MLP and ELP-enriched fraction among total BM cells are shown. (G) Rag1/GFP heterozygous mice with or without the sFRP5 transgene were obtained by mating Rag1/GFP homozygous males and sFRP5-TG females. At 10 weeks of age, BM cells were collected and analyzed using flow cytometry. The LSK fraction was gated and further resolved using Rag1/GFP and Flt3 intensities. Numbers in each panel represent percentages of the Flt3$^-$ Rag1/GFP$^-$ HSC-enriched, Flt3$^+$ Rag1/GFP$^-$ MLP, or Flt3$^+$ Rag1/GFP$^+$ ELP fractions among the LSK cells and are shown as averages with SD ($n = 3$ in each). Data are representative of two independent experiments, with similar results. (H) Frequencies and cell counts of the Lin$^-$ c-kit^{lo} Sca1$^{-/lo}$ Flt3$^+$ IL-7Rα^+ CLP fraction in whole BM are shown. Statistically significant differences are indicated by p values. (I) Lin$^-$ c-kit^{lo} Sca1$^{-/lo}$ Flt3$^+$ IL-7Rα^+ CLPs were obtained from WT or sFRP5-TG mice and cultured in stromal cell-free serum-free conditions. After 7 days of culture, recovered cells were counted and analyzed by flow cytometry. Absolute numbers of recovered cells were divided by the numbers of CLPs used to initiate the cultures to obtain the yield per input values shown in the left graph. (C, D, F, H, and I) Data are shown as mean ± SEM and are representative of three independent experiments.

© 2015 WILEY-VCH Verlag GmbH & Co. KGaA, Weinheim

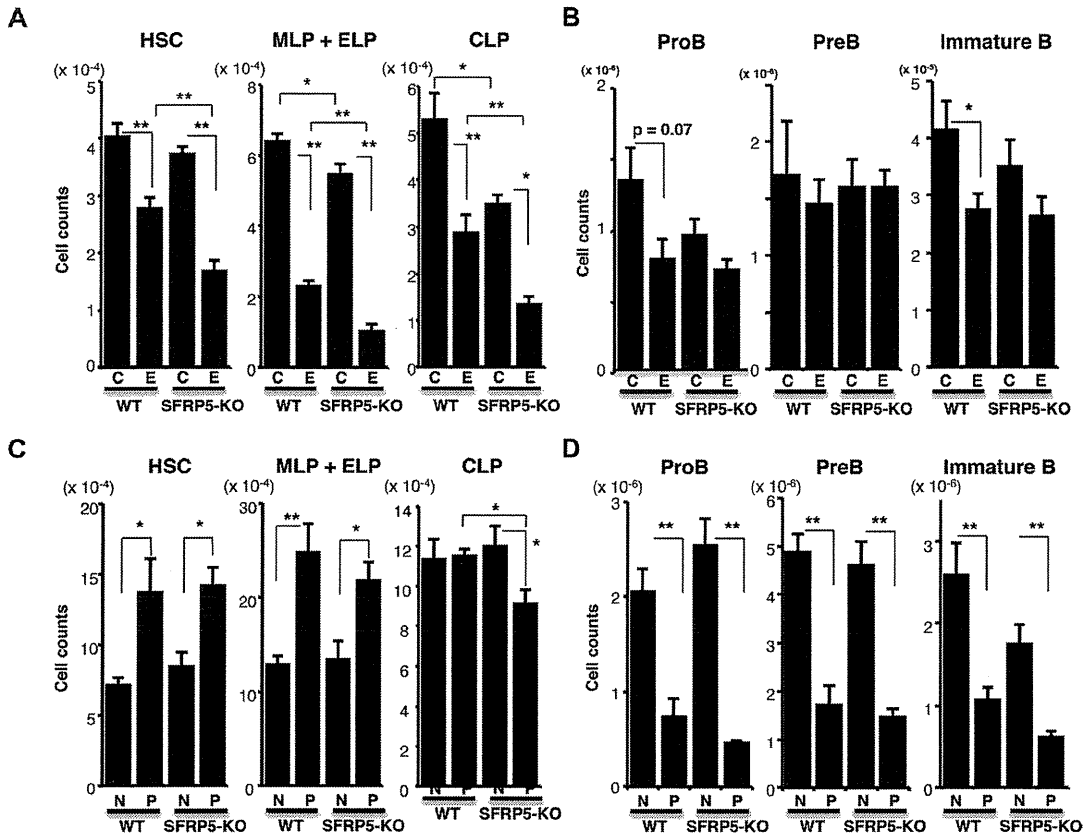

Figure 5. SFRP5 deficiency influences early lympho-hematopoiesis in vivo. (A, B) β-Estradiol dissolved in saline (E) or saline alone (C) was intraperitoneally injected into WT or sFRP5-KO mice (7–8 weeks old) for four consecutive days. Control mice were treated with saline alone. The mice were killed 12 h after the last injection, and the extent of B-lymphopoiesis was evaluated. Early stages of lympho-hematopoiesis, including LSK Flt3$^-$ HSCs, LSK Flt3$^+$ MLPs, and ELPs, and CLPs (A) and late stages of B-lymphopoiesis in BM, including ProB, PreB, and immature B cells (B) were examined with or without β-estradiol. The frequency of each fraction was determined by flow cytometry and multiplied by the absolute cell counts obtained from two long bones (one femur and one tibia). ($n = 7$ in each group). (C, D) WT females (10 weeks of age) were mated with WT males, and sFRP5-KO females (10 weeks of age) were mated with sFRP5-KO males. Mice that had been successfully mated but were subsequently found not to be pregnant were used as controls. N: not pregnant P: pregnant ($n = 5$, WT not pregnant; $n = 5$, WT pregnant; $n = 7$, sFRP5-KO not pregnant; and $n = 5$, sFRP5-KO pregnant). Early stages of lympho-hematopoiesis (C) and late stages of B-lymphopoiesis in BM (D) were evaluated as described above. Data are shown as mean + SEM and are representative of two independent experiments. ($^*p < 0.05$, $^{**}p < 0.01$; unpaired two-tailed t-tests).

Frizzled receptors independently of Wnts [11, 33, 34], structural CRD differences among sFRPs could change their association pattern to target proteins, consequently resulting in different biological activities. In fact, while sFRP1, sFRP2, and sFRP5 are functionally redundant in embryonic development [16], sFRP1 and sFRP2 substantially differ with respect to their activity on HSCs and multipotent progenitors [21]. Thus, within the sFRP family, sFRP5 may have discrete roles in B-lymphopoiesis. To address this important issue, sophisticated experimental strategies that enable the evaluation of in vivo associations among diverse sFRPs, Frizzled receptors, and Wnts are required.

Our study focused on the function of BM stromal cells to uncover factors involved in extrinsic regulation of B-lymphopoiesis. The present data clearly show that environmental sFRP5 affects HSCs and early B-lymphopoiesis in response to high estrogen levels. During the preparation of this manuscript, Nakada et al. reported that estrogen and pregnancy enhance HSC division and myelo-erythropoiesis in mice [35]. Interestingly, they demonstrated that estrogen directly influences HSC division via estrogen receptor-α (ER-α) in female mice but not male mice. We identified sFRPs as estrogen-inducible molecules in BM stromal cells via ER-α [7]. Our group also observed that the frequency and absolute number of HSCs significantly increased in the BM of pregnant mice at the expense of B-lymphoid progenitors (Fig. 5C–D), which is consistent with the results of Nakada et al. Estrogen may directly induce sFRPs or other related molecules in HSCs. Cell intrinsic and extrinsic mechanisms are not mutually exclusive, and we propose that estrogen and pregnancy affect HSCs not only in a direct manner but also by affecting BM stromal cells. Indeed, Nakada et al. demonstrated that the deletion of ER-α from hematopoietic cells reduces HSC numbers in the spleen but not in the BM of pregnant mice [35]. This observation indicates that some environmental factors in the BM compensate for ER-α deficiency of HSCs during pregnancy.

In summary, we identified a novel mechanism in which estrogen-inducible sFRP5 strongly blocks B-lymphopoiesis.

© 2015 WILEY-VCH Verlag GmbH & Co. KGaA, Weinheim

However, high sFRP5 or even high estrogen cannot explain by themselves the pregnancy-related changes in the immune system. Although the amount of sFRP5 in our transgenic model is probably higher than the physiological level obtained during pregnancy, high sFRP5 levels did not recapitulate pregnancy-related changes in many aspects. During pregnancy or estrogen treatment, T- and B-lymphopoiesis is significantly suppressed, whereas sFRP5 overexpression was found to mainly suppress B-lymphopoiesis. Pregnancy or estrogen treatment in vivo significantly reduces Rag1/GFP$^+$ ELPs in the BM [7], but these cells are preserved in sFRP5-TG mice. Furthermore, significant reduction of HSCs, as well as MLPs + ELPs and CLPs, in sFRP5-KO mice treated with estrogen indicates that sFRP5 deescalates the exhaustion of HSCs and primitive lymphoid progenitors caused by high estrogen levels. While sFRP5 preserves these primitive stem/progenitor cells by counteracting the massive impact of estrogen, the same protein strongly inhibits the later stages of B-lineage differentiation. Pregnancy involves elaborate and complex mechanisms for maintaining maternal–fetal immune tolerance, of which only some of this tolerance can be attributed to sFRPs. Nevertheless, we believe that our findings on estrogen-inducible sFRP5 will be helpful in clinical medicine by providing baseline data to develop a new immune-modulatory method in the future.

Materials and methods

Animals

SFRP-TG mice were generated using a previously described method [15] and backcrossed with the C57BL6/J strain more than eight times. SFRP5-deficient mice and Rag1/GFP knock-in mice were previously established [16, 36]. WT C57BL/6 mice were obtained from CLEA Japan Inc. (Tokyo, Japan). The animal experiments were designed according to the guidelines established by the animal committee of Osaka University and the design was approved by the ethics review board (permission number 21-011-016).

Antibodies

Rabbit polyclonal antibodies to sFRP1 and sFRP5 were obtained from abcam (ab4193; Cambridge, MA) and Sigma-Aldrich (HPA019840; St. Louis, MO), respectively. FITC-anti-Mac1 (M1/70), Gr-1 (Ly-6G; RB6-8C5), erythroid (TER-119), CD8a (53-6.7), CD19 (1D3), CD45R/B220 (RA3/6B2), CD5 (53-7.3), IgM (R6-60.2), CD34 (RAM34), PE-anti-Mac1, CD19, CD45R/B220, CD5, and c-kit (2B8) MoAbs were obtained from BD Biosciences (San Diego, CA). FITC-anti-CD3 (145-2c11), PE-anti-CD43 (1B11), IgD (11-26c, 2a), IL7Ra (SB/199), and Flt3 (A2F10), Biotin-anti-CD23 (B3B4), IL7Ra, Flt3 MoAb, PE/Cy7-anti-CD93 (AA4.1), allophycocyanin-anti-CD45R/B220, and c-kit MoAbs were purchased from BioLegend (San Diego, CA). Purified anti-Mac1, Gr-1, TER-119-erythroid, CD3 (145-2C11), CD45RA (14.8), and CD19 MoAbs obtained from BD Biosciences were used for depleting lineage-related marker (Lin)$^+$ cells, followed by incubation with goat anti-rat IgG-coated magnetic beads (Miltenyi Biotec, Auburn, CA).

Flow cytometry and cell sorting

Cells were stained with fluorescence-conjugated MoAbs and analyzed using FACSCanto or FACSAria (BD Biosciences). HSCs, MLPs, ELPs, CLPs, ProB, PreB, and immature B cells were identified based on previously established criteria [19, 20, 37–39]. Adult BM cells from sFRP5-TG mice and their WT littermates were used to isolate Lin$^-$ c-kit^{lo} Sca-1^{lo} Flt3$^+$ IL7Rα^+ CLPs [20]. In some experiments, adult BM cells from sFRP5-deficient mice were used to sort LSK cells and CLPs.

Methylcellulose colony-forming assay

BM cells were prepared from 5–6-week-old sFRP5-TG mice and their WT littermates. The cells were cultured in Iscove's Modified Dulbecco's Medium-based methylcellulose medium supplemented with 1 ng/mL of recombinant mouse (rm) IL-7 (Methocult M3630; StemCell Technologies, Canada) or 50 ng/mL of rm SCF, 10 ng/mL of rm IL-3, 10 ng/mL of recombinant human IL-6, and 3 units/mL of recombinant human erythropoietin (Methocult GF3434) at a concentration of 5×10^5 cells/mL or 5×10^4 cells/mL, respectively. The number of colony-forming progenitors responding to IL-7 (CFU PreB) and CFU myeloerythroid cells were enumerated after seven and nine days, respectively.

Stromal cell-free serum-free lymphocyte culture

CLPs were isolated from 5–6-week-old sFRP5-TG mice and their WT littermates, cultured in 24-well culture plates (5000 cells/well) with SF-03 medium (Sanko-Junyaku, Japan) containing 1% bovine serum albumin, 50 μM 2-mercaptoethanol, 2 mM L-glutamine, 1 ng/mL rm IL-7, 100 ng/mL rm Flt3-ligand, and 20 ng/mL rm SCF, and fed on the fourth day of culture. After 7 days, cells were counted and analyzed by flow cytometry.

Statistical methods

Unpaired, two-tailed *t*-tests were used for intergroup comparisons, and p values were considered significant if they were less than 0.05. Error bars used throughout indicate SEM.

© 2015 WILEY-VCH Verlag GmbH & Co. KGaA, Weinheim

Acknowledgments: Phylogenetic analyses were performed with the computing system at Genome Information Research Center, Osaka University. This work was supported by the New Energy and Industrial Technology Development Organization (NEDO) (funding recipients; K.T., K.Y., and M.K), JSPS KAKENHI Grant Number 21591241 (funding recipients; T.Y., K.O., and Y.K.) and JSPS KAKENHI Grant Number 25461450 (funding recipients; K.F., T.Y., K.O., and Y.K.). Author contributions; T.Y. conducted experiments and analyzed results; T.Y., K.O., P.W.K., and Y.K. designed the research plan and wrote the manuscript; T.S., T.I., Y.D., and Y.H. prepared mouse cells and performed the flow cytometry; M.I., K.F., and D.O. performed gene expression analyses; K.T., K.Y., and M.K. established sFRP transgenic mice; A.S. established sFRP5-deficient mice; E.M. prepared murine tissue sections and performed histological assessment. We thank Dr. Ouchi (Nagoya University) and Dr. Kamada (Osaka University) for transferring the sFRP5-deficient mice.

Conflict of interest: The authors declare no financial or commercial conflict of interest.

References

1 Medina, K. L., Smithson, G. and Kincade, P. W., Suppression of B Lymphopoeisis during Nomial Pregnancy. *J. Exp. Med.* 1993. **178**: 1507–1515.

2 Rijhsinghani, A. G., Bhatia, S. K., Tygrett, L. T. and Waldschmidt, T. J., Effect of Pregnancy on Thymic T Cell Development. *Am. J. Reprod. Immunol.* 1996. **35**: 523–528.

3 Medina, K. L. and Kincade, P. W., Pregnancy-related steroids are potential negative regulators of B lymphopoiesis. *Proc. Natl. Acad. Sci. USA* 1994. **91**: 5382–5386.

4 Smithson, G., Medina, K. L., Ponting, I. and Kincade, P. W., Estrogen suppresses stromal cell-dependent lymphopoiesis in culture. *J. Immunol.* 1995. **155**: 3409–3417.

5 Kincade, P. W., Medina, K. L., Payne, K. J., Rossi, M. I., Tudor, K., Yamashita, Y. and Kouro, T., Early B-lymphocyte precursors and their regulation by sex steroids. *Immunol. Rev.* 2000. **175**: 128–137.

6 Kincade, P. W., Lymphoid lineage cells in adult murine bone marrow diverge from those of other blood cells at an early, hormone-sensitive stage. *Semin. Immunol.* 2002. **14**: 385–394.

7 Yokota, T., Oritani, K., Garrett, K. P., Kouro, T., Nishida, M., Takahashi, I., Ichii, M. et al., Soluble frizzled-related protein 1 is estrogen inducible in bone marrow stromal cells and suppresses the earliest events in lymphopoiesis. *J. Immunol.* 2008. **181**: 6061–6072.

8 Kawano, Y. and Kypta, R., Secreted antagonists of the Wnt signalling pathway. *J. Cell Sci.* 2003. **116**: 2627–2634.

9 Esteve, P., Sandonis, A., Ibanez, C., Shimono, A., Guerrero, I. and Bovolenta, P., Secreted frizzled-related proteins are required for Wnt/beta-catenin signalling activation in the vertebrate optic cup. *Development* 2011. **138**: 4179–4184.

10 Renström, J., Istvanffy, R., Gauthier, K., Shimono, A., Mages, J., Jardon-Alvarez, A., Kröger, M. et al., Secreted Frizzled-related protein 1 extrinsically regulates cycling activity and maintenance of hematopoietic stem cells. *Cell Stem Cell* 2009. **5**: 157–167.

11 Dann, C. E., Hsieh, J.-C., Rattner, A., Sharma, D., Nathans, J. and Leahy, D. J., Insights into Wnt binding and signalling from the structures of two Frizzled cysteine-rich domains. *Nature* 2001. **412**: 86–90.

12 Clevers, H., Wnt/β-catenin signaling in development and disease. *Cell* 2006. **127**: 469–480.

13 Staal, F. J. T., Luis, T. C. and Tiemessen, M. M., WNT signalling in the immune system: WNT is spreading its wings. *Nat. Rev. Immunol.* 2008. **8**: 581–593.

14 Lee, H. X., Ambrosio, A. L., Reversade, B. and DeRobertis, E. M., Embryonic dorsal-ventral signaling: secreted frizzled-related proteins as inhibitors of tolloid proteinases. *Cell* 2006. **124**: 147–159.

15 Kakitani, M., Oshima, T., Horikoshi, K., Yoshitome, T., Ueda, A., Kajikawa, M., Iba, Y. et al. A novel transgenic chimaeric mouse system for the rapid functional evaluation of genes encoding secreted proteins. *Nucleic Acids Res.* 2005. **33**: e85–e85.

16 Satoh, W., Matsuyama, M., Takemura, H., Aizawa, S. and Shimono, A., Sfrp1, Sfrp2, and Sfrp5 regulate the Wnt/beta-catenin and the planar cell polarity pathways during early trunk formation in mouse. *Genesis* 2008. **46**: 92–103.

17 Allman, D. and Pillai, S., Peripheral B cell subsets. *Curr. Opin. Immunol.* 2008. **20**: 149–157.

18 Hardy, R. R., B-1 B cells: development, selection, natural autoantibody and leukemia. *Curr. Opin. Immunol.* 2006. **18**: 547–555.

19 Hardy, R. R., Kincade, P. W. and Dorshkind, K., The protean nature of cells in the B lymphocyte lineage. *Immunity* 2007. **26**: 703–714.

20 Kondo, M., Weissman, I. L. and Akashi, K., Identification of clonogenic common lymphoid progenitors in mouse bone marrow. *Cell* 1997. **91**: 661–672.

21 Nakajima, H., Ito, M., Morikawa, Y., Komori, T., Fukuchi, Y., Shibata, F., Okamoto, S. and Kitamura, T., Wnt modulators, SFRP-1, and SFRP-2 are expressed in osteoblasts and differentially regulate hematopoietic stem cells. *Biochem. Biophys. Res. Comm.* 2009. **390**: 65–70.

22 Fleming, H. E., Janzen, V., Lo Celso, C., Guo, J., Leahy, K. M., Kronenberg, H. M. and Scadden, D. T., Wnt signaling in the niche enforces hematopoietic stem cell quiescence and is necessary to preserve self-renewal in vivo. *Cell Stem Cell* 2008. **2**: 274–283.

23 Malhotra, S. and Kincade, P. W., Wnt-related molecules and signaling pathway equilibrium in hematopoiesis. *Cell Stem Cell* 2009. **4**: 27–36.

24 Luis, T. C., Naber, B. A., Roozen, P. P., Brugman, M. H., de Haas, E. F., Ghazvini, M., Fibbe, W. E. et al., Canonical wnt signaling regulates hematopoiesis in a dosage-dependent fashion. *Cell Stem Cell* 2011. **9**: 345–356.

25 Leyns, L., Bouwmeester, T., Kim, S. H., Piccolo, S. and DeRobertis, E. M., Frzb-1 is a secreted antagonist of Wnt signaling expressed in the Spemann organizer. *Cell* 1997. **88**: 747–756.

26 Wang, S., Krinks, M., Lin, K., Luyten, F. P. and Moos, M., Jr., Frzb, a secreted protein expressed in the Spemann organizer, binds and inhibits Wnt-8. *Cell* 1997. **88**: 757–766.

27 Lin, K., Wang, S., Julius, M. A., Kitajewski, J., Moos, M., Jr. and Luyten, F. P., The cysteine-rich frizzled domain of Frzb-1 is required and sufficient for modulation of Wnt signaling. *Proc. Natl. Acad. Sci. USA* 1997. **94**: 11196–11200.

28 Rodriguez, J., Esteve, P., Weinl, C., Ruiz, J. M., Fermin, Y., Trousse, F., Dwivedy, A., Holt, C. and Bovolenta, P., SFRP1 regulates the growth of

© 2015 WILEY-VCH Verlag GmbH & Co. KGaA, Weinheim

retinal ganglion cell axons through the Fz2 receptor. *Nat. Neurosci.* 2005. 8: 1301–1309.

29 Kobayashi, K., Luo, M., Zhang, Y., Wilkes, D. C., Ge, G., Grieskamp, T., Yamada, C. et al., Secreted Frizzled-related protein 2 is a procollagen C proteinase enhancer with a role in fibrosis associated with myocardial infarction. *Nat. Cell Biol.* 2009. 11: 46–55.

30 He, W., Zhang, L., Ni, A., Zhang, Z., Mirotsou, M., Mao, L., Pratt, R. E. and Dzau, V. J., Exogenously administered secreted frizzled related protein 2 (Sfrp2) reduces fibrosis and improves cardiac function in a rat model of myocardial infarction. *Proc. Natl. Acad. Sci. USA* 2010. 107: 21110–21115.

31 Esteve, P., Sandonis, A., Cardozo, M., Malapeira, J., Ibanez, C., Crespo, I., Marcos, S. et al., SFRPs act as negative modulators of ADAM10 to regulate retinal neurogenesis. *Nat. Neurosci.* 2011. 14: 562–569.

32 Xavier, C. P., Melikova, M., Chuman, Y., Uren, A., Baljinnyam, B. and Rubin, J. S., Secreted Frizzled-related protein potentiation versus inhibition of Wnt3a/beta-catenin signaling. *Cell. Signal.* 2014. 26: 94–101.

33 Bafico, A., Gazit, A., Pramila, T., Finch, P. W., Yaniv, A. and Aaronson, S. A., Interaction of frizzled related protein (FRP) with Wnt ligands and the frizzled receptor suggests alternative mechanisms for FRP inhibition of Wnt signaling. *J. Biol. Chem.* 1999. 274: 16180–16187.

34 Carron, C., Pascal, A., Djiane, A., Boucaut, J. C., Shi, D. L. and Umbhauer, M., Frizzled receptor dimerization is sufficient to activate the Wnt/beta-catenin pathway. *J. Cell Sci.* 2003. 116: 2541–2550.

35 Nakada, D., Oguro, H., Levi, B. P., Ryan, N., Kitano, A., Saitoh, Y., Takeichi, M. et al., Oestrogen increases haematopoietic stem-cell self-renewal in females and during pregnancy. *Nature* 2014. 505: 555–558.

36 Kuwata, N., Igarashi, H., Ohmura, T., Aizawa, S. and Sakaguchi, N., Absence of expression of RAG1 in peritoneal B-1 cells detected by knocking into RAG1 locus with green fluorescent protein gene. *J. Immunol.* 1999. 163: 6355–6359.

37 Medina, K. L., Strasser, A. and Kincade, P. W., Estrogen influences the differentiation, proliferation, and survival of early B-lineage precursors. *Blood* 2000. 95: 2059–2067.

38 Adolfsson, J., Månsson, R., Buza-Vidas, N., Hultquist, A., Liuba, K., Jensen, C. T., Bryder, D. et al., Identification of Flt3+ lympho-myeloid stem cells lacking erythro-megakaryocytic potential. *Cell* 2005. 121: 295–306.

39 Igarashi, H., Gregory, S. C., Yokota, T., Sakaguchi, N. and Kincade, P. W., Transcription from the RAG1 locus marks the earliest lymphocyte progenitors in bone marrow. *Immunity* 2002. 17: 117–130.

Abbreviations: **BM**: bone marrow · **CLP**: common lymphoid progenitor · **ELP**: early lymphoid progenitor · **HSC**: hematopoietic stem cell · **LSK**: Lin^- $Sca\text{-}1^+$ $c\text{-}kit^{hi}$ · **Lin**: lineage-related markers · **MLP**: multilineage progenitor · **Sfrp**: secreted Frizzled-related protein · **Wnt**: Wingless and Int-1

Full correspondence: Dr. Takafumi Yokota, Department of Hematology and Oncology, Osaka University Graduate School of Medicine, C9, 2-2 Yamada-oka, Suita, Osaka 565-0871, Japan
e-mail: yokotat@bldon.med.osaka-u.ac.jp
Fax: 81-6-6879-3879

Received: 13/6/2014
Revised: 11/1/2015
Accepted: 10/2/2015
Accepted article online: 13/2/2015

© 2015 WILEY-VCH Verlag GmbH & Co. KGaA, Weinheim

We have shown that transcriptional noise is well predicted by molecularly detailed models for the two most common promoter architectures in *E. coli* as the various genetic knobs are tuned. This agreement is not the result of fitting theory curves to data, because the predicted curves are generated using physical parameter values reported elsewhere in the literature and in that sense are zero-parameter predictions. Earlier reports of "bursty" transcription (*5*, *21*) are based on the observation that the Fano factor is greater than 1 for constitutive mRNA production (as well as direct kinetic measurements). Various explanatory hypotheses have been proposed, including transcriptional silencing via DNA condensation by nucleoid proteins (*22*), negative supercoiling induced by transcription, or the formation of long-lived "dead-end" initiation complexes (*23*). Although our data do not rule out these hypotheses, we find that extrinsic noise is sufficient to explain the deviation from Fano = 1 in our constitutive expression data (Fig. 2B). Thus, we find no need to invoke alternative hypotheses to explain the observed "burstiness" of constitutive transcription.

Many interesting earlier experiments make it difficult to interpret differences between promoters and induction conditions in terms of distinct physical parameters because of the wide variety of promoter architectures in play as well as the diverse mechanisms of induction. We have instead taken a "synthetic biology" approach of building promoters from the ground up. By directly controlling aspects of the promoter architecture, our goal has been to directly relate changes in promoter architecture to changes in observed gene expression variability. We believe that this work has demonstrated that mutations in regulatory DNA can alter gene expression noise. This suggests that gene expression noise may be a tunable property subject to evolutionary selection pressure, as mutations in regulatory DNA could provide greater fitness by increasing (or decreasing) variability. Demonstrating the relevance of this hypothesis in natural environments remains an ongoing challenge.

REFERENCES AND NOTES

1. J. Paulsson, M. Ehrenberg, *Phys. Rev. Lett.* **84**, 5447–5450 (2000).
2. A. Sanchez, H. G. Garcia, D. Jones, R. Phillips, J. Kondev, *PLOS Comput. Biol.* **7**, e1001100 (2011).
3. Y. Taniguchi *et al.*, *Science* **329**, 533–538 (2010).
4. W. J. Blake *et al.*, *Mol. Cell* **24**, 853–865 (2006).
5. L. H. So *et al.*, *Nat. Genet.* **43**, 554–560 (2011).
6. H. Salman *et al.*, *Phys. Rev. Lett.* **108**, 238105 (2012).
7. H. Maamar, A. Raj, D. Dubnau, *Science* **317**, 526–529 (2007).
8. A. Eldar, M. B. Elowitz, *Nature* **467**, 167–173 (2010).
9. G. M. Süel, R. P. Kulkarni, J. Dworkin, J. Garcia-Ojalvo, M. B. Elowitz, *Science* **315**, 1716–1719 (2007).
10. M. Thattai, A. van Oudenaarden, *Genetics* **167**, 523–530 (2004).
11. E. Kussell, S. Leibler, *Science* **309**, 2075–2078 (2005).
12. H. Salgado *et al.*, *Nucleic Acids Res.* **41**, D203–D213 (2013).
13. L. Bintu *et al.*, *Curr. Opin. Genet. Dev.* **15**, 125–135 (2005).
14. T. Kuhlman, Z. Zhang, M. H. Saier Jr., T. Hwa, *Proc. Natl. Acad. Sci. U.S.A.* **104**, 6043–6048 (2007).
15. J. M. Vilar, S. Leibler, *J. Mol. Biol.* **331**, 981–989 (2003).
16. See supplementary materials on *Science* Online.
17. A. Sánchez, J. Kondev, *Proc. Natl. Acad. Sci. U.S.A.* **105**, 5081–5086 (2008).
18. P. S. Swain, M. B. Elowitz, E. D. Siggia, *Proc. Natl. Acad. Sci. U.S.A.* **99**, 12795–12800 (2002).
19. R. C. Brewster, D. L. Jones, R. Phillips, *PLOS Comput. Biol.* **8**, e1002811 (2012).
20. P. Hammar *et al.*, *Science* **336**, 1595–1598 (2012).
21. I. Golding, J. Paulsson, S. M. Zawilski, E. C. Cox, *Cell* **123**, 1025–1036 (2005).
22. A. Sanchez, S. Choubey, J. Kondev, *Annu. Rev. Biophys.* **42**, 469–491 (2013).
23. N. Mitarai, I. B. Dodd, M. T. Crooks, K. Sneppen, *PLOS Comput. Biol.* **4**, e1000109 (2008).

ACKNOWLEDGMENTS

We thank H. J. Lee, C. Wiggins, Y. Lin, X. Zhu, F. Weinert, M. Rydenfelt, R. Milo, H. Garcia, N. Belliveau, and J. Sheung for useful discussions. Supported by NIH grants DP1 OD000217 (Directors Pioneer Award), R01 GM085286, and 1 U54 CA143869 (Northwestern PSOC Center); La Fondation Pierre Gilles de Gennes (R.P.); and the Donna and Benjamin M. Rosen Center for Bioengineering at Caltech (D.L.J.). Raw microscopy image data are archived in the Phillips laboratory at Caltech and are available upon request.

SUPPLEMENTARY MATERIALS

www.sciencemag.org/content/346/6216/1533/suppl/DC1
Materials and Methods
Supplementary Text
Figs. S1 to S11
Tables S1 to S3
References (*24–32*)

28 April 2014; accepted 4 November 2014
10.1126/science.1255301

IMMUNE TOLERANCE

Detection of self-reactive CD8$^+$ T cells with an anergic phenotype in healthy individuals

Yuka Maeda,[1] Hiroyoshi Nishikawa,[1]* Daisuke Sugiyama,[1] Danbee Ha,[1] Masahide Hamaguchi,[1] Takuro Saito,[1] Megumi Nishioka,[1,2] James B. Wing,[1] Dennis Adeegbe,[1] Ichiro Katayama,[2] Shimon Sakaguchi[1]*

Immunological tolerance to self requires naturally occurring regulatory T (T_{reg}) cells. Yet how they stably control autoimmune T cells remains obscure. Here, we show that T_{reg} cells can render self-reactive human CD8$^+$ T cells anergic (i.e., hypoproliferative and cytokine hypoproducing upon antigen restimulation) in vitro, likely by controlling the costimulatory function of antigen-presenting cells. Anergic T cells were naïve in phenotype, lower than activated T cells in T cell receptor affinity for cognate antigen, and expressed several coinhibitory molecules, including cytotoxic T lymphocyte–associated antigen-4 (CTLA-4). Using these criteria, we detected in healthy individuals anergic T cells reactive with a skin antigen targeted in the autoimmune disease vitiligo. Collectively, our results suggest that T_{reg} cell–mediated induction of anergy in autoimmune T cells is important for maintaining self-tolerance.

Naturally occurring CD25$^+$CD4$^+$ regulatory T (T_{reg}) cells, which specifically express the transcription factor FoxP3, actively maintain immunological self-tolerance and homeostasis (*1*). Developmental or functional anomalies of natural T_{reg} cells can cause autoimmune diseases (such as type I diabetes), allergy, and immunopathological diseases (such as inflammatory bowel disease) (*1*). How T_{reg} cells effectively control potentially hazardous self-reactive T cells in humans remains an open question. In particular, it is unknown whether T_{reg} cell–mediated suppression for a limited period has a critical long-lasting effect on cell fate and antigen reactivity of autoimmune T cells.

To address this issue, we examined proliferation, cytokine production, and cell fate of antigen-specific CD8$^+$ T cells in peripheral blood mononuclear cells (PBMCs) from healthy individuals stimulated in vitro with self-antigen peptide in the presence or absence of natural FoxP3$^+$CD25$^+$CD4$^+$ T_{reg} cells. Melan-A (also known as MART-1) used in the experiments is a self-antigen expressed by normal melanocytes and some melanoma cells and targeted in vitiligo vulgaris, an autoimmune disease of the skin (*2–5*). In the absence of T_{reg} cells, Melan-A–specific CD8$^+$ T cells [detectable by major histocompatibility complex (MHC) tetramers and peptide tetramers] expanded over 10 days from very few cells to a sizable fraction when cultured with peptide-pulsed autologous antigen-presenting cells (APCs) (Fig. 1A) (*6*). Natural T_{reg} cells, which appeared to be activated by endogenous self-peptides and class II MHC on autologous APCs (*7–9*), suppressed the expansion of Melan-A tetramer–positive (Tet$^+$) CD8$^+$ T cells in a dose-dependent manner. Similar stimulation with irrelevant peptide NY-ESO-1, another self- and tumor antigen, failed to induce Melan-ATet$^+$CD8$^+$ T cells. In cultures containing T_{reg} cells,

[1]Experimental Immunology, Immunology Frontier Research Center (IFReC-WPI), Osaka University, Osaka 565-0871, Japan. [2]Department of Dermatology, Graduate School of Medicine, Osaka University, Osaka 565-0871, Japan.
*Corresponding author. E-mail: shimon@ifrec.osaka-u.ac.jp (S.S.); nisihiro@ifrec.osaka-u.ac.jp (H.N.)

Downloaded from www.sciencemag.org on December 18, 2014